Annales Geophysicae

The role of bromine and chlorine chemistry for arctic ozone depletion events in Ny-Ålesund and comparison with model calculations

M. Martinez, T. Arnold, D. Perner

Max-Planck-Institut für Chemie, Becherweg 27, D-55128 Mainz
E-mail: martinez@mpch-mainz.mpg.de

Abstract. During the Arctic Tropospheric Ozone Chemistry (ARCTOC) campaigns at Ny-Ålesund, Spitsbergen, the role of halogens in the depletion of boundary layer ozone was investigated. In spring 1995 and 1996 up to 30 ppt bromine monoxide were found whenever ozone decreased from normal levels of about 40 ppb. Those main trace gases and others were specifically followed in the UV-VIS spectral region by differential optical absorption spectroscopy (DOAS) along light paths running between 20 and 475 m a.s.l.. The daily variation of peroxy radicals closely followed the ozone photolysis rate $J(O_3(O^1D))$ in the absence of ozone depletion most of the time. However, during low ozone events this close correlation was no longer found because the measurement of radicals by chemical amplification (CA) turned out to be sensitive to peroxy radicals and ClO_x. Large CA signals at night can sometimes definitely be assigned to ClO_x and reached up to 2 ppt. Total bromine and iodine were both stripped quantitatively from air by active charcoal traps and measured after neutron activation of the samples. Total bromine increased from background levels of about 15 ppt to a maximum of 90 ppt during an event of complete ozone depletion. For the spring season a strong source of bromine is identified in the pack ice region according to back trajectories. Though biogenic emission sources cannot be completely ruled out, a primary activation of halogenides by various oxidants seems to initiate an efficient autocatalytic process, mainly driven by ozone and light, on ice and perhaps on aerosols. Halogenides residing on pack ice surfaces are continuously oxidised by hypohalogenous acids releasing bromine and chlorine into the air. During transport and especially above open water this air mixes with upper layer pristine air. As large quantities of bromine, often in the form of BrO, have been observed at polar sunrise also around Antarctica, its release seems to be a natural phenomenon. The source strength of bromine from halogen activation on the pack ice, as

based on the measured inorganic bromine levels, averages about 10^{12} Br-atoms $m^{-2} s^{-1}$ during sunlit periods in Arctic spring. The total source strength of inorganic bromine from sunlit polar regions may therefore amount to 30 kt y^{-1}.

Key words. Atmospheric composition and structure (troposphere – composition and chemistry; instruments and techniques).
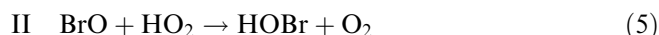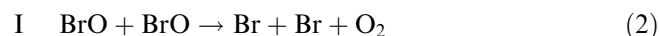
1 Introduction

Berg *et al.* (1983) reported average mixing ratios of 130 ppt for total atmospheric bromine during peak periods in the Arctic (Pt. Barrow, Alaska, and Ny-Ålesund, Spitsbergen) from mid-February until mid-May for several years of observation compared to normal levels of 15 ppt. Then low ozone events, LOEs, were observed regularly during spring in the boundary layer at Pt. Barrow (Oltmans and Komhyr, 1986) and at Alert, Canada (Bottenheim *et al.*, 1986). Barrie *et al.* (1989, 1988) found "filterable" bromine, mostly Br^-, to be negatively correlated with ozone and they related the ozone depletion directly to the inorganic bromine. These findings were confirmed in detailed Arctic investigations (Mickle *et al.*, 1989; Bottenheim *et al.*, 1990; Sturges *et al.*, 1993, Barrie *et al.*, 1994). Boundary LOEs were also found at Ny-Ålesund, Spitsbergen, and at Søndre Stømfjord and Thule, both in Greenland (Mikkelsen *et al.*, 1996; Solberg *et al.*, 1996). Recently LOEs were identified around Antarctica at Syowa, 69°S, 39°E (Murayama *et al.*, 1992) and at G. v. Neumayer station, 70°S, 8°W (Wessel *et al.*, 1998), where anthropogenic influences are much scarcer than in the Arctic.

The Polar Sunrise Experiment 1992 (Barrie *et al.*, 1994) led to the observation of bromine monoxide, BrO,

Correspondence to: M. Martinez

by long-path differential optical absorption spectroscopy (DOAS) at Alert (Hausmann and Platt, 1994). In the follow up experiment 1995/96 on Arctic Tropospheric Ozone Chemistry (ARCTOC, 1997) a number of groups investigated the influence of halogens upon tropospheric ozone at Ny-Ålesund. Spectroscopic results on BrO and ClO have been published by Tuckermann *et al.* (1997) and Martinez (1998). Simultaneous observations by ground-based zenith sky DOAS confirmed the existence of tropospheric BrO (Wittrock *et al.*, 1996). Similar observations by the same method were reported from Søndre Strømfjord, Greenland (Miller *et al.*, 1997), and from Arrival Heights, 77.8°S, 166.7°E, Antarctica (Kreher *et al.*, 1997; Kreher, 1996). Ozone reacts quickly with halogen atoms see Eq. (1).
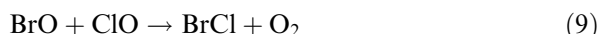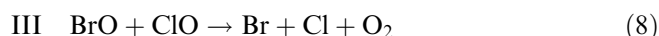
$$X + O_3 \rightarrow XO + O_2 \qquad (X = Cl, Br, I) \qquad (1)$$

Bromine by itself destroys ozone through catalytic cycles I and II

$$
\begin{aligned}
\text{I} \quad & BrO + BrO \rightarrow Br + Br + O_2 & (2) \\
& \qquad\qquad\quad \rightarrow Br_2 + O_2 & (3) \\
& Br_2 + h\nu \quad \rightarrow Br + Br & (4) \\
\text{II} \quad & BrO + HO_2 \rightarrow HOBr + O_2 & (5) \\
& HOBr + h\nu \rightarrow OH + Br & (6)
\end{aligned}
$$

followed by reaction (1) and (7).

$$OH + O_3 \rightarrow HO_2 + O_2 \qquad (7)$$

The synergistic action of bromine and chlorine (cycle III) destroys ozone as well (McElroy *et al.*, 1986).

$$
\begin{aligned}
\text{III} \quad & BrO + ClO \rightarrow Br + Cl + O_2 & (8) \\
& BrO + ClO \rightarrow BrCl + O_2 & (9) \\
& BrO + ClO \rightarrow Br + OClO & (10) \\
& BrCl + h\nu \quad \rightarrow Br + Cl & (11) \\
& OClO + h\nu \rightarrow O + ClO & (12)
\end{aligned}
$$

The source of the photochemically active bromine in the atmosphere could be gasphase photolysis or oxidation of organobromides (CH_3Br, $CHBr_3$, etc.) (Schauffler *et al.*, 1998). Yokouchi *et al.* (1994) observed detailed negative correlations of $CHBr_3$ and O_3 during LOEs. However, total atmospheric bromine during LOEs exceeds by far that of known organobromides which also photodissociate comparatively slowly. In addition a rapid formation of hydrobromic acid, HBr, from active bromine in gasphase photochemical cycles was pointed out by McConnell *et al.* (1992).

Oxidation of condensed phase bromides or HBr to gas phase bromine could solve this inconsistency (McConnell *et al.*, 1992; Tang and McConnell, 1996). Finlayson-Pitts *et al.* (1990) proposed the surface oxidation of Br^- by dinitrogenpentoxide, while Fan and Jacob (1992) propagated the heterogeneous oxidation of HBr by hypobromous acid, HOBr (Eigen and Kustin, 1962), on ice or aerosol surfaces see Eq. (13).

$$HOBr + H^+ + Br^- \rightarrow H_2O + Br_2 \qquad (13)$$
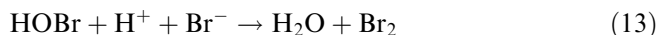
Mozurkewitch (1995) considered the oxidation of aqueous bromide by peroxymonosulfuric acid (Caro's acid) as well as by OH and HO_2. According to Wessel (1996) and Wessel *et al.* (1997) the oxidant could be H_2O_2. Sander and Crutzen (1996) proposed oxidation of bromide by OH and NO_3 radicals in deliquesced sea-salt aerosols. Recently a process by which bromine is released in a dark process through O_3 oxidation of sea salt was described by Oum *et al.* (1998a) and Hirokawa *et al.* (1998).

Contrary to those relatively inefficient processes, the autocatalytic release, as firstly proposed by Mozurkewitch (1995), can provide a rapid increase in atmospheric bromine concentration by emissions from sea-salt. Thereby HOBr formed in reactions (1)–(5) oxidises HBr by heterogeneous reaction (13). A detailed oxidation mechanism was discussed by Vogt *et al.* (1996). Tang and McConnell (1996) proposed the autocatalytic release of bromine explicitly from sea-salt bromide on the snow of the Arctic pack ice. The efficiency of this process was experimentally verified by Kirchner *et al.* (1997) who observed the release of BrCl and Br_2 from sea-salt on ice. Interestingly the rate of this process increases at lower pH (Fickert *et al.*, 1998; Behnke *et al.*, 1998).

The participation of chlorine in arctic ozone destruction and in halogen release was shown by the changing hydrocarbon pattern during LOEs (Jobson *et al.*, 1994). For the ARCTOC campaigns such an involvement of chlorine was also found (Ramacher *et al.*, 1997; Rudolph *et al.*, 1997; see also ARCTOC, 1997).

Chlorine may be released from aqueous sea-salt in the presence of ozone and light (Oum *et al.*, 1998b), though Impey *et al.* (1997) report an observation of Cl_2 in the dark before Arctic sunrise. The participation of chlorine invokes synergistic ozone destruction via a coupling of BrO/ClO (McElroy *et al.*, 1986) according to cycle III. The significance of this cycle in comparison to cycles I, II was discussed by Le Bras and Platt (1995).

Mixing ratios of up to 600 ppt formaldehyde were observed around LOEs by de Serves (1994). Such high levels may be generated from oxidation of hydrocarbons in the ice phase but may also indicate the involvement of chlorine atoms in the oxidation of hydrocarbons.

Here new results for BrO and ClO as well as for related compounds from the ARCTOC campaigns at Ny-Ålesund, Spitsbergen, in spring of 1995 and 1996 are presented.

2 Experimental

2.1 DOAS

Measurements of O_3, BrO, ClO, IO, SO_2, NO_2, OClO and HCHO were carried out in Ny-Ålesund on the west coast of Spitsbergen (78.9°N, 11.8°E) by active long path DOAS observation. The instrumental setup described by Platt and Perner (1983) allows trace gas concentrations to be determined from their narrow

absorption bands in the UV-VIS spectral region. Light from a white light source (Hanovia L5269, Xe-arc) was directed along a path of several kilometres through the atmosphere, collected at the end and dispersed by a spectrograph. The differential optical densities of the absorption bands yielded integrated concentrations for the air volume covered. For a detailed description of the DOAS technique see Platt (1994).

In 1995 the light path was installed between the main building of the North Polar Institute (20 m a.s.l.) and Zeppelin mountain (474 m a.s.l., 2100 m distance). The measurements were carried out with a Czerny-Turner spectrograph (resolution 0.45 nm) and a photomultiplier detector. A 30 nm part of the spectrum in the focal plane was consecutively scanned by $100\,\mu m$ slits (Ladstätter-Weißenmayer, 1992). The light was collected for 400 s and from the integrated spectrum a background spectrum taken immediately afterwards was subtracted. For that purpose the focus of the incoming lamp beam was shifted away from the entrance slit.

In 1996, retroreflectors were placed again on Zeppelin mountain and in addition also on Bøggerfjellet (410 m a.s.l., 5000 m distance). The spectrograph equipped with a holographic grating (resolution 0.9 nm) and a photodiode array detector allowed simultaneous recording of a much wider section of the spectrum (Martinez, 1998). The pixel to pixel diode variation of the array was corrected by the multi-channel-scanning technique (MCST) (Brauers *et al.*, 1995). For that purpose a sequence of 19 spectra, each background corrected, was taken, and within this sequence every spectrum was shifted by 0.7 nm in wavelength with respect to the foregoing. The exposure time for a single spectrum was about 30 s and in a first step all those spectra were summed up according to array pixel numbering. Thus the structures caused by the individual sensitivities of the photodiodes are preserved in the sum while spectral features are smoothed out and the pixel to pixel variation can be taken out by dividing each individual spectrum by that spectral sum. The final spectrum is produced by adding all spectra after reshifting each divided spectrum back to its original position. Examples of such final atmospheric spectra are shown in Figs. 1 and 2 for the two spectral regions. Narrow bands remain almost unaltered by the MCST application, while wider bands are reduced.

The trace gas column densities along the light path were derived from their proper absorbances which are determined from a simultaneous least-squares fit of the reference spectra of all trace compounds and of a polynomial to the air spectrum (Stutz, 1995). The reference spectra for O_3, SO_2, NO_2 and HCHO were obtained from quartz cells with the particular gas placed in the light path. SO_2 and NO_2 cells were filled permanently. Solid paraformaldehyde was heated to release gaseous HCHO, and O_3 was produced at the measuring site by flowing oxygen through a silent discharge. Halogen oxide spectra recorded before in the laboratory were wavelength-calibrated according to the NO_2 spectrum. BrO had been produced by irradiating mixtures of Br_2 and ozone with 254 nm mercury
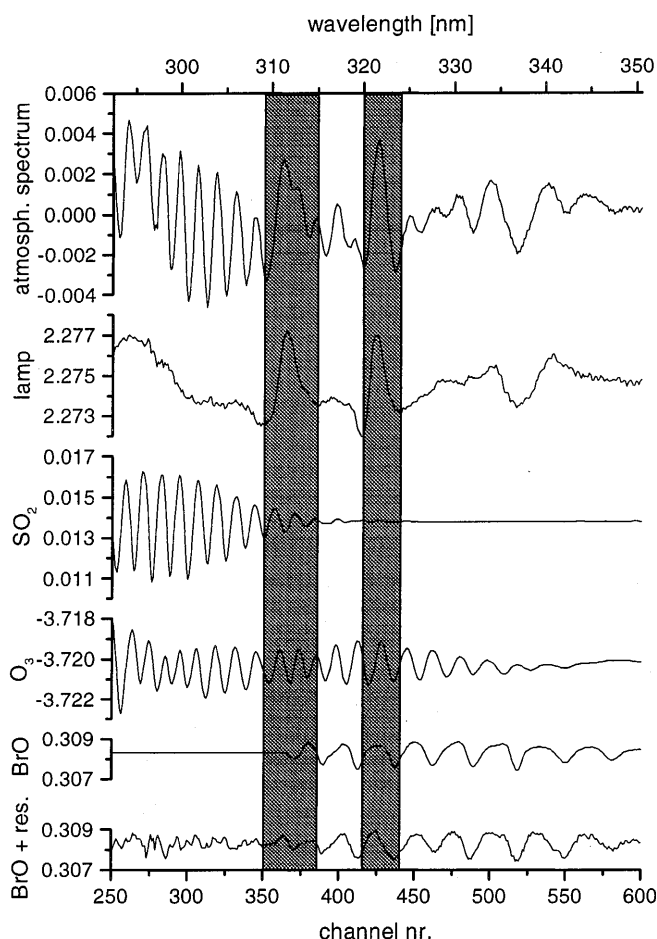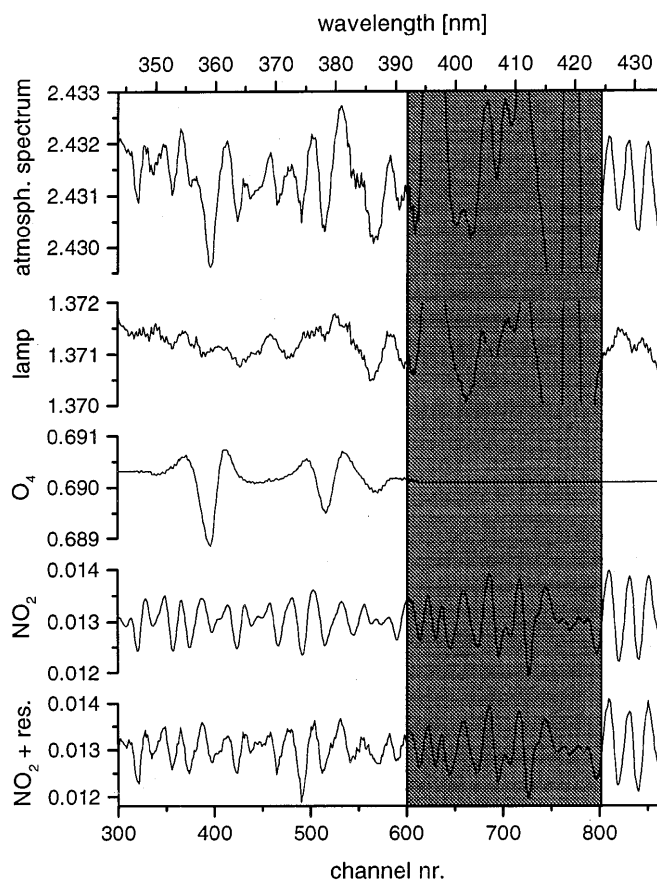

Fig. 1. Air spectrum in the wavelength region 293–350 nm, path length 4200 m (*trace a*). The fitted spectral absorption intensities correspond to atmospheric trace gas absorptions of 30 ppb O_3 (*d*), 1 ppb SO_2 (*c*) and 9 ppt BrO (*e*). The *shaded areas* cover large lamp structures (*b*) and were excluded from the fit. *Trace f* shows the atmospheric BrO spectrum obtained from the air spectrum by taking out the fitted lamp structures and species absorptions of SO_2 and O_3

light (Philips TUV 40 W). For IO a literature spectrum had to be used. Examples for O_3, SO_2 and BrO spectra are given in Fig. 1 together with a field spectrum. Figure 2 shows an example for the spectral region of the NO_2 absorption at longer wavelength. The lamp structures and absorptions by atmospheric O_4 are also given in both figures.

The differential absorption cross sections required for the calculation of concentrations were obtained by folding the higher-resolution cross sections (references see Table 1) with Hg-line spectra as measured by the instrument. The temperature dependencies of the spectra of O_3, BrO and SO_2 were taken into account. The actual value for the BrO differential absorption cross section at 338 nm was 1.5×10^{-17} cm^2 at 253 K for the spectrograph used in 1995 and 9.2×10^{-18} cm^2 at 263 K for the instrument used in 1996. Application of MCST diminished the latter value to 9.1×10^{-18} cm^2.

The systematic errors derived for the concentrations are caused mainly by lamp structures (the main limitation of detection) and by uncertainties of the absorption coefficients (3–20%). Statistical errors arise from photon

Fig. 2. Air spectrum in the wavelength region 344–434 nm for the evaluation of NO_2, path length 4200 m (*trace a*). Lamp spectrum (*b*), O_4 spectrum (*c*) and atmospheric absorption by 1.35 ppb NO_2 (*d*). The *shaded area* was excluded from the fit because of large lamp structures. *Trace e* shows the atmospheric NO_2 spectrum obtained from the air spectrum by taking out the fitted lamp structures and the species absorption of O_4

Table 1. Wavelengths and detection limits for DOAS

Species	Wavelength of prominent band, nm	Detection limit 1995	Detection limit 1996	Literature absorption coefficients
O_3	299	5 ppb	2 ppb	Bass and Paur, 1984
BrO	338	5 ppt	2 ppt	Wahner *et al.*, 1988
ClO	295	50 ppt	25 ppt	Simon *et al.*, 1990
IO	427	4 ppt	2 ppt	Laszlo *et al.*, 1995
OClO	336		2 ppt	Wahner *et al.*, 1987
SO_2	300	150 ppt	50 ppt	McGee and Burris, 1987
NO_2	349, 431	500 ppt 280 ppt	250 ppt 140 ppt	Schneider *et al.*, 1987
HCHO	338	1.3 ppb	500 ppt	Moortgat *et al.*, 1989
HONO	342		100 ppt	Bongartz *et al.*, 1991, 1994

statistics, from detector noise and from random residual instrument structures.

2.2 Air sample collection

In 1996 total bromine and total iodine were collected from air by drawing ambient air through cartridges (12 mm diameter, 45 mm length) filled with activated charcoal (Carbo-Act Interntl.) at a flow rate of $0.7 \, m^3/h$. The air volume was followed by a dry gas meter at the exit of the pump and the temperature was measured there as well as outside. During strong LOEs sampling times were reduced to 12 h from 24 h at normal O_3 levels. The sampling efficiency for all bromine and iodine compounds was assumed as unity. After neutron activation of the charcoal samples the emissions of the isotopes Cl^{38}, Br^{80} and I^{128} were measured.

The original charcoal contained no bromine as confirmed by blank samples and also by samples used in the field when the air throughput was reduced unintentionally by snow. However, the charcoal was contaminated by some iodine and this average background was subtracted from all samples.

For calibration fresh charcoal samples were spiked with solutions containing $1 \, \mu g \, Br^-$ and $1 \, \mu g \, I^-$ and treated by identical neutron activation procedures. The detection limit was 6 ng Br/sample (0.5 ppt in $6 \, m^3$ air) and 5 ng I/sample (0.3 ppt in $6 \, m^3$ air), with a precision of about 10%.

2.3 RO_x-box

During both campaigns a chemical amplifier, commonly called RO_x-box, followed peroxy radical mixing ratios (Cantrell *et al.*, 1984; Hastie *et al.*, 1991; Arnold, 1998). This chemical amplification is based on the OH/HO_2 radical catalysed chain oxidation of CO to CO_2 and NO to NO_2 see Eqs. (14)–(16) as initiated by HO_x and RO_x radicals.

$$HO_2 + NO \rightarrow NO_2 + OH \tag{14}$$
$$OH + CO \rightarrow CO_2 + H \tag{15}$$
$$H + O_2 + M \rightarrow HO_2 + M \tag{16}$$
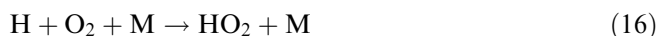
The number of cycles, e.g. the amplification, is calibrated with known amounts of HO_2 radicals and by measuring the product NO_2. Organic peroxy radicals are converted to HO_2 first by reactions (17)–(19). The contributions of OH and alkoxy are usually negligible in comparison to that of RO_2/HO_2.

$$RO_2 + NO \rightarrow NO_2 + RO \tag{17}$$
$$RO + O_2 \rightarrow R'CHO + HO_2 \tag{18}$$
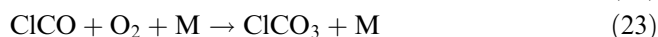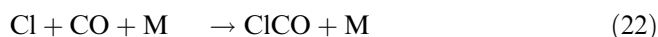$$\rightarrow R''\text{-CO-}R''' + HO_2 \tag{19}$$
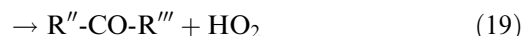
The chain can be terminated by wall losses and by the combination of OH and HO_2. The main loss of the radicals is probably the formation of HONO see Eq. (20).

$$OH + NO + M \rightarrow HONO + M \qquad (20)$$
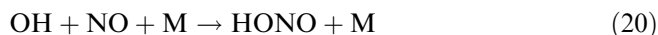
The efficiency of the chain reaction, i.e. the number of NO_2 molecules produced from one primary radical, is called chain length, CHL and shortens with increasing water vapour pressure as recently found by Mihele and Hastie (1998). The instrument (Arnold, 1998) was placed 1.5 km southwest of the village centre at an altitude of 50 m a.s.l. on the snow-covered ground.

The RO_x/HO_x mixing ratios were expected to follow the daily variation of the radiative flux, as observed for example from the beginning of the campaign to April 6, 1996 (Fig. 8). Yet during LOEs (Fig. 9), when less RO_x/HO_x were expected on the basis of reduced rates of radical formation from ozone photolysis, the RO_x-box signal showed rather high values. At night it exceeded zero during LOEs (Fig. 9) substantially. Therefore laboratory investigations on other possibly interfering radicals were started which revealed a chain oxidation of NO to NO_2 by chlorine oxides, ClO, OClO and chlorine atoms, Cl (Perner et al., 1999).

$$ClO + NO \qquad \rightarrow Cl + NO_2 \qquad (21)$$

$$Cl + CO + M \qquad \rightarrow ClCO + M \qquad (22)$$

$$ClCO + O_2 + M \rightarrow ClCO_3 + M \qquad (23)$$

$$ClCO_3 + NO \qquad \rightarrow Cl + CO_2 + NO_2 \qquad (24)$$

These reactions have been described before by Hewitt et al. (1996). The chain may be terminated by the combination of Cl with NO:

$$Cl + NO + M \rightarrow ClNO + M \qquad (25)$$

The signal of the peroxy experiment therefore goes back to the oxidation of NO to NO_2 by the combined action of RO_x/HO_x and ClO_x. The corresponding bromine species have no effect.

The chemiluminescence response of the luminol detector (LMA/3, Scintrex) was calibrated with known NO_2 concentrations from permeation tubes in dry air. Starting in 1996, 25 ppb NO_2 were added to the gas flow just before the detector in order to reach its linear response region (Hastie et al., 1991).

CHL is determined for reactions (14)–(20) by

$$CHL_{perox} = \frac{[NO_2]_{on} - [NO_2]_{off}}{[HO_2] + [RO_2]} \qquad (26)$$

and for reactions (21)–(25) by

$$CHL_{chl} = \frac{[NO_2]_{on} - [NO_2]_{off}}{[Cl] + [ClO]} \qquad (27)$$

where $[NO_2]_{on}$ denotes the resulting NO_2 concentration with the amplification switched on and $[NO_2]_{off}$ denotes that with the amplification switched off.

The chainlength for peroxy radicals CHL_{perox} was calibrated by photolysis of a mixture of water vapour and synthetic air at 185 nm (Brune et al., 1995; Schultz et al., 1995) at regular intervals at the field site. The average CHL_{perox} in dry air was found as $160 \pm 15 \, (1\sigma)$ in 1995 and $155 \pm 10 \, (1\sigma)$ in 1996. These values agree quite well with calibration results obtained with dry air

in the laboratory at Mainz. The instrumental reproducibility (precision) based upon calibration was 6%. The uncertainty (accuracy) of the measurements, which had been determined during an intercalibration experiment to $\pm 20\%$ (see also Hofzumahaus et al., 1997), must now be considered as $+100\% - 20\%$, since Mihele and Hastie (1998) reported the radical amplification to depend on moisture. From March to the beginning of May the temperatures were below freezing so that the error from disregarding the dependence on water vapour might then be small.

The calibration for chlorine was carried out with known concentrations of OClO in air. After dynamic dilution to 86 ppt a chain length of 300 ± 60 was found (Perner et al., 1998). To date nothing is known about the possible influence of water vapour on the length of the chlorine chain. With respect to the low solubility of chlorine compounds in water no dramatic influence of water vapour as compared to the RO_x/HO_x cycle is expected.

The detection limit was 2 and 1 ppt for RO_x/HO_x (10-min-average) and 1 and 0.5 ppt for ClO_x in 1995 and 1996, respectively. In cases when both RO_x/HO_x and ClO_x coexisted the signal cannot be unambiguously assigned to either RO_x/HO_x or ClO_x. For analysis of the field data the RO_x-box signals were converted to theoretical RO_x/HO_x mixing ratios with a CHL_{perox} of 155. Under circumstances when the signal is only due to ClO_x (e.g. at night) its mixing ratio is 1/2 of that (155/300).

During the 1996 campaign $J\left(O_3\left(O^1D\right)\right)$ was followed by two 2π-sr filter radiometers (Meteorologie Consult) pointing up- and downwards (Junkermann et al., 1989). A recent validation improved the uncertainty quoted by the company to about $\pm 10\%$.

3 Results

During spring, the boundary air at Ny-Ålesund normally contained 40–45 ppb of O_3, while BrO remained below the detection limit of 2–5 ppt. When BrO rose above the detection limit it was associated with LOEs and negatively correlated to O_3 (Figs. 3, 4, 6, 7). As long as some O_3 was left and reaction (1) could proceed, BrO was found. The mixing layer height measured by balloon sondes in Ny-Ålesund during LOEs was between 500 and 2000 m (ARCTOC, 1997). Mixing ratios of ClO, IO, OClO, CH_2O and HONO always remained under their spectroscopic detection limits by DOAS (Table 1). Yet a few ppt of ClO_x were signalled by the more sensitive RO_x-box during LOEs and sometimes even in the absence of any ozone depletion. The signals of the RO_x-box are presented as RO_x/HO_x mixing ratios according to the calibration by HO_2 (Figs. 5, 8, 9). Under favourable conditions an unambiguous identification of ClO_x could be made from RO_x-box signals.

3.1 Campaign 1995

The pack-ice field was close to Svalbard. Our measurements started on April 20 in the middle of a LOE.
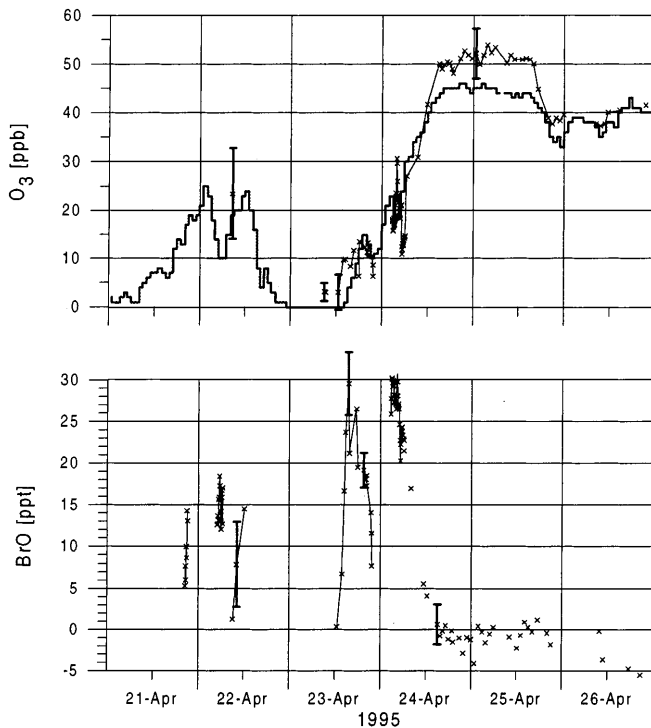
Fig. 3. ARCTOC 1995: mixing ratios of O_3 at Zeppelin Station (Monitor Lab, *solid line*), and of O_3 and BrO measured by DOAS (*crosses*) during a low ozone event

Before noon on April 23 O_3 was zero and BrO was also undetectable (Fig. 3). In the afternoon an air mass arrived with 10 to 15 ppb O_3 and BrO was up to 30 ppt. Around noon on April 24 BrO disappeared and the O_3
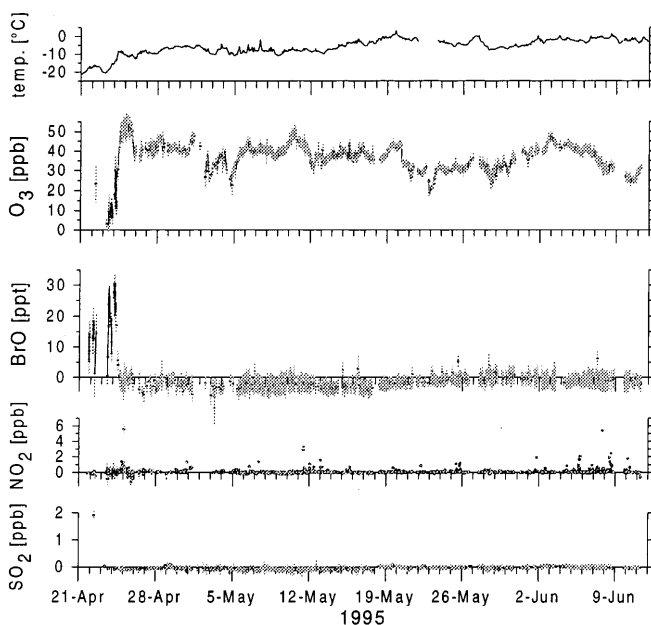
Fig. 4. ARCTOC 1995: all data of O_3, BrO, NO_2 and SO_2 measured by DOAS during the campaign and temperature at Zeppelin station (ARCTOC, 1997)

recovered to 50 ppb. Then the total active bromine was probably very low again. The 2σ error limit of DOAS for O_3 was 5 ppb and no significant deviation from the values of the ozone monitor at Zeppelin station was observed, indicating in general a uniform distribution with altitude.

Figure 4 shows the temperature and mixing ratios for O_3, BrO, NO_2 and SO_2 from DOAS. The latter two were mostly below their respective detection limits, as well as CH_2O and $OClO$ (Table 1). On April 22 two ppb of SO_2 were observed together with BrO. Frequent spikes in NO_2 were probably due to local pollution.

The signals from the RO_x-box which started to operate on May 1 (Fig. 5) frequently showed no correlation with the diurnal variation of the radiative flux, indicated by the photolysis rate for NO_2, $J(NO_2)$. The highest signals in May corresponded to 10 ppt RO_x/HO_x and large signals were frequent at night, which may have indicated the presence of ClO_x. In June the signals did not exceed 5 ppt RO_x/HO_x and even under sunny conditions on June 1 the signal levels were not as high as on May 8, 9, 10.

3.2 Campaign 1996

At this time approximately 200 km of open water separated the pack-ice from Ny-Ålesund. BrO and O_3 by DOAS are shown in Fig. 6, together with total bromine and iodine from neutron activation. BrO and O_3 were again negatively correlated during LOEs but BrO mixing ratios were generally lower than in 1995. Total bromine was 10 to 20 ppt during periods of undisturbed ozone and increased during LOEs.

SO_2 was observed on several occasions, mostly during LOEs (Fig. 6). On April 14–18 under conditions of calm weather the SO_2 showed levels around 300 ppt with little variation, which were also observed by Staebler on Zepellinfjellet (ARCTOC, 1997). In the
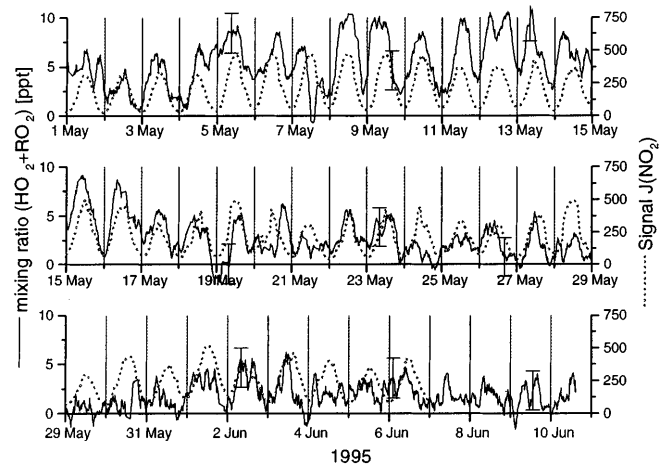
Fig. 5. ARCTOC 1995: RO_x-box signals (*solid line*) calibrated corresponding to $RO_x + HO_x$ together with $J(NO_2)$ from Zeppelin Station (*dotted line*)
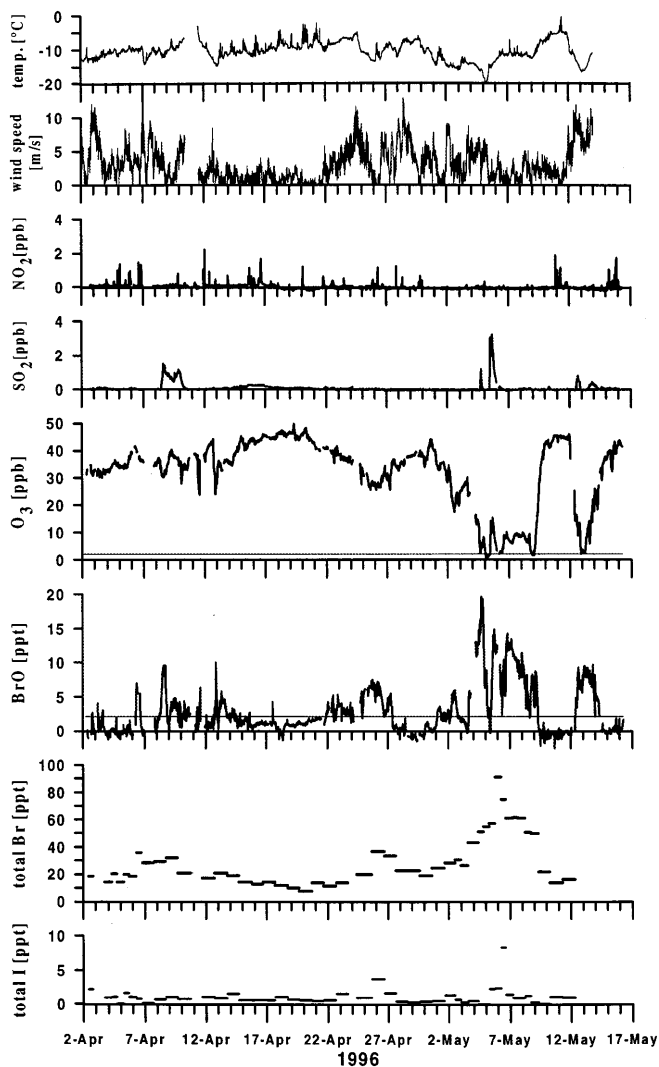
Fig. 6. ARCTOC 1996: all data of NO_2, SO_2, O_3 and BrO measured by DOAS during the campaign together with temperature and wind speed at Zeppelin station (ARCTOC, 1997). Total bromine and iodine collected on active charcoal and measured by neutron activation analysis

afternoon of May 5 the air, with up to 2 ppb SO_2, very likely had come a long distance as the SO_2 correlates closely with O_3 and shows no correlation with NO_2.

The NO/NO_2 instrument on Zeppelin mountain operated by NILU (ARCTOC, 1997) showed only spikes of up to 400 ppt NO_2 throughout the campaign. NO_2 spikes from our DOAS observations (Fig. 6) and those measured by DOAS Heidelberg some km north-west of Ny-Ålesund often reached 1–3 ppb during both campaigns and were much more frequent (ARCTOC, 1997), the Heidelberg concentrations being generally higher than those obtained by us. The missing correlation between the DOAS and NILU NO_2 observations indicates that the NO_2 originated from local pollution. Furthermore the NO_2 spikes appeared to be reduced during LOEs probably due to the slower conversion rate of the local NO emissions to NO_2 by the smaller O_3 concentrations.

In the beginning of the campaign the RO_x-box signals in Fig. 8 followed the daily radiative intensity reasonably well up to April 6 when the first observation of BrO was made (Fig. 6). From then total bromine increased and peroxy radical signals became higher. Those high peroxy radical signals at day and night together with the displacement of the daily maximum away from noon (Fig. 8) eventually led to the detection of the chlorine response of the RO_x-box (Perner *et al.*, 1999). On April 14–19 the RO_x-box signals were also surprisingly high, though the O_3 was not visibly affected, probably indicating ClO_x (Fig. 8) during this period.

Two major LOEs were encountered on May 4–9 and May 12–14 (Fig. 6). The first LOE is depicted in more detail in Fig. 7. Total bromine increased to 60 ppt and higher while BrO was 15–20 ppt. IO was not detected even on May 6 when 8 ppt total iodine exceeded the normal level of 1–2 ppt (Fig. 6). In between the two LOEs (May 10 and 11) the RO_x-box signals returned to a normal behaviour probably indicating the presence of RO_x/HO_x only (Fig. 8).

The second LOE, May 12–14 1996 (Figs. 6, 9), was dominated by strong winds (ARCTOC, 1997). 7–10 ppt BrO accompanied the decreasing O_3 from the beginning around midnight May 11/12 until the morning of May 14 (Fig. 6). The RO_x-box signals, probably mainly due to ClO_x, jumped up around midnight and decreased later during the day (Fig. 9).

At the end of the LOEs the BrO disappeared a few hours before the O_3 returned to normal 40–45 ppb. In 1995 no such delay between the disappearance of BrO and the recovery of O_3 was observed.

The O_3 mixing ratios were linearly and negatively correlated with total bromine (Fig. 10). At a given O_3 level the BrO mixing ratio varied highly. Yet the highest BrO mixing ratios were negatively correlated with the O_3 mixing ratio above 5 ppb, reaching a maximum of 20 ppt BrO at about 5 ppb O_3 and then decreasing with lower O_3 mixing ratios (Fig. 11).

4 Discussion

The springtime boundary layer O_3 destruction appears to be a complex phenomenon which bears on several aspects of air chemistry:

1. Volatilisation of halogen from halides on pack ice surfaces and aerosol surfaces by heterogeneous oxidations
2. Gasphase halogen chemistry
3. The influence of emissions from polar regions on the global tropospheric inorganic bromine budget.

The identification of active chlorine, ClO_x, by chemical amplification allowed its direct measurement in the Arctic boundary for the first time. This data together with the BrO data obtained during LOEs provides the means for further investigation on active halogen formation and the associated O_3 destruction. The vertical mixing height of depleted O_3 above Ny-Ålesund
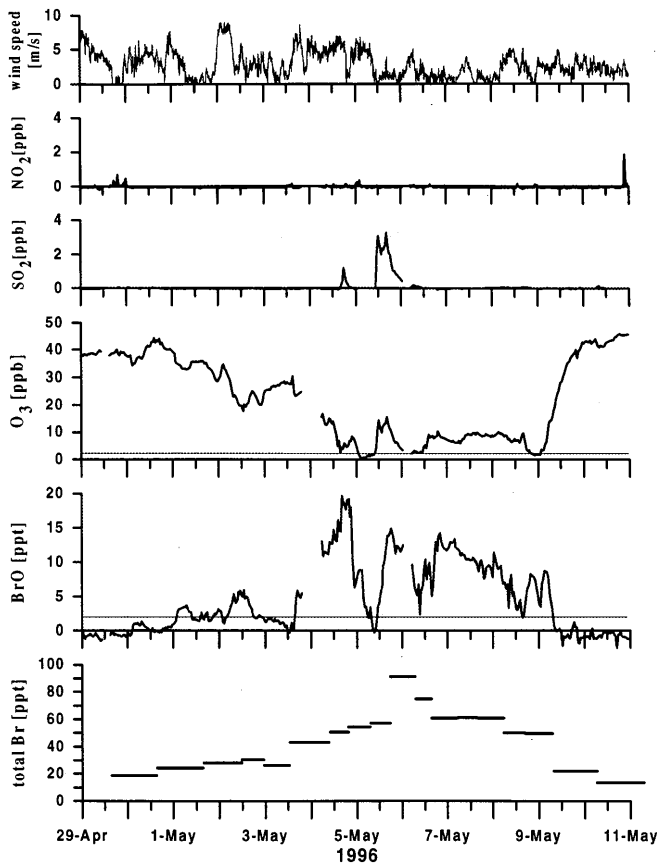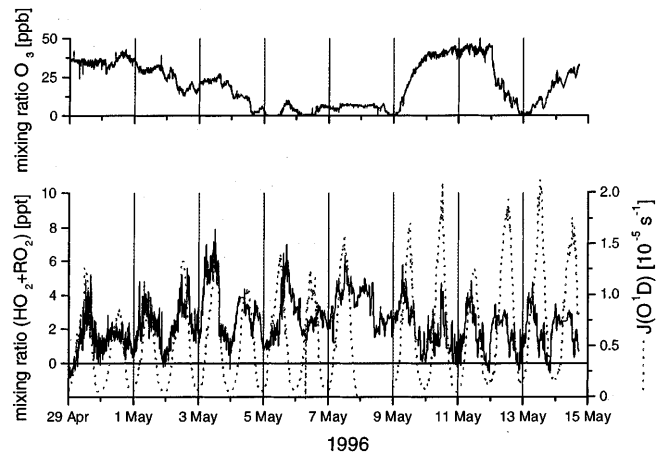
Fig. 7. The main ozone depletion event, ARCTOC 1996: mixing ratios of NO_2, SO_2, O_3 and BrO measured by DOAS together with wind speed at Zeppelin station (ARCTOC, 1997) and total bromine from neutron activation analysis

was about twice in 1996 compared to 1995. This probably relates to stronger turbulent mixing of the air during its transport from the central pack ice region over open water compared to over the ice layer (ARCTOC, 1997).
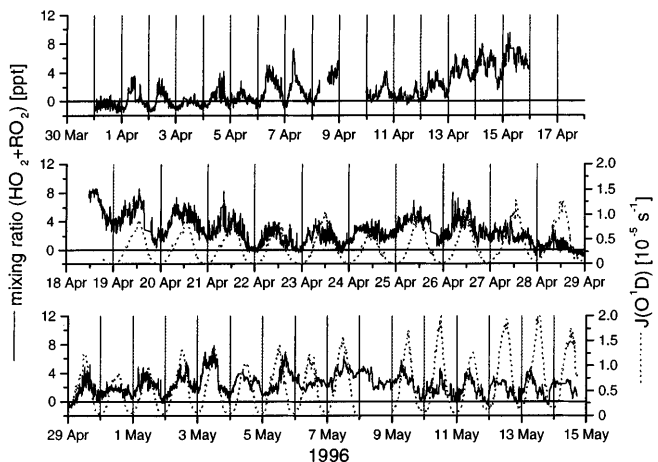
Fig. 8. ARCTOC 1996: RO_x-box signals (*solid line*) calibrated corresponding to $RO_x + HO_x$ and $J(O_3(O^1D))$ (*dotted line*)

Fig. 9. The main ozone depletion event, ARCTOC 1996: O_3, RO_x-box signals (calibrated corresponding to $RO_x + HO_x$, *solid line*) and $J(O_3(O^1D))$ (*dotted line*)
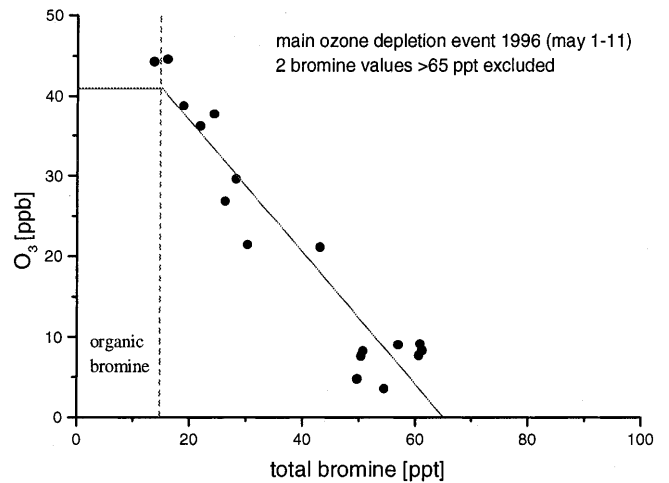
Fig. 10. O_3 mixing ratio as function of total bromine, main ozone depletion event 1996
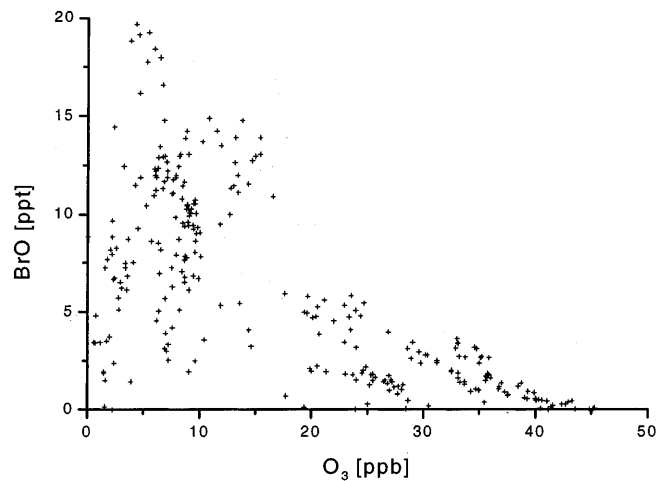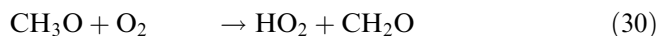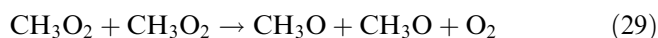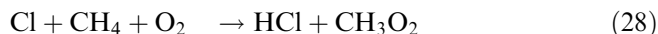

Fig. 11. BrO mixing ratio as function of O_3 mixing ratio, main ozone depletion event 1996

4.1 Active halogens

Chlorine and bromine atoms react with O_3 (reaction 1) to form ClO and BrO. While Br atoms cannot abstract hydrogen from alkanes, part of the Cl atoms react with hydrocarbons to yield stable hydrochloric acid, HCl, and a peroxy radical (Eq. 28). In the case of methane the methylperoxy radical is formed, which is a precursor of formaldehyde (Eqs. 29, 30).

$$Cl + CH_4 + O_2 \quad \rightarrow HCl + CH_3O_2 \qquad (28)$$

$$CH_3O_2 + CH_3O_2 \rightarrow CH_3O + CH_3O + O_2 \qquad (29)$$

$$CH_3O + O_2 \qquad \rightarrow HO_2 + CH_2O \qquad (30)$$

Br atoms are easily formed in the self-reaction of BrO (Eq. 2). Br-atoms cannot abstract hydrogen from alkanes, but HBr is eventually formed via reactions (31) and (32). Depending on the amount of CH_2O present the lifetime of active bromine is of the order of hours. The active bromine is reformed from HBr via reaction (13).

$$Br + HO_2 \quad \rightarrow HBr + O_2 \qquad (31)$$

$$Br + CH_2O \rightarrow HBr + HCO \qquad (32)$$

The channels for BrO do not exist for ClO. Only a small amount of the ClO resides in the dimer, $(ClO)_2$, according to the equilibrium at ambient temperatures. Consequently ClO is fairly stable under Arctic conditions, its main loss being the reactions with BrO and with HO_2, the latter yielding HOCl (reaction 33) which photolyses easily (Eq. 34).

$$ClO + HO_2 \rightarrow HOCl + O_2 \qquad (33)$$

$$HOCl + h\nu \rightarrow Cl + OH \qquad (34)$$
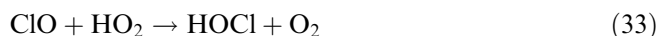
During LOEs, when BrO is present, one major reaction channel (Eq. 10) leads to formation of OClO. Cl atoms are generated directly (Eq. 8) or indirectly via BrCl (Eqs. 9, 11). The lifetime of Cl atoms against reaction with methane (Eq. 28) is about 0.5 s. HCl may be heterogeneously oxidised by HOBr or HOCl on ice surfaces (Eqs. 35, 36, similar to reaction 13) to yield molecular halogens

$$HCl + HOBr \rightarrow BrCl + H_2O \qquad (35)$$

$$HCl + HOCl \rightarrow Cl_2 + H_2O \qquad (36)$$

which are then photolysed (Eqs. 11, 37) to regenerate halogen atoms.

$$Cl_2 + h\nu \rightarrow Cl + Cl \qquad (37)$$

4.1.1 DOAS.
The measurements of halogen monoxides, ClO, BrO and IO, in this work by long path optical absorption showed only BrO. Tuckermann *et al.* (1997) reported average mixing ratios of 21 and 3.3 ppt ClO for the LOE periods in 1995 and 1996, respectively, by a frequency analysis of their DOAS observations.

The mixing ratios of formaldehyde remained always below the detection limit of 500 ppt in 1996 (1.3 ppb in 1995). In the solar sunrise experiment 1992 de Serves

(1994) had observed up to 700 ppt formaldehyde during LOEs.

HONO was not detected by us. However, Staebler reported the detection of HONO by denuder on a few occasions (ARCTOC, 1997).

4.1.2 RO_x-box.
The sensitivity of the RO_x-box for ClO_x is higher than of DOAS for ClO and sufficient to measure the few ppt of ambient ClO_x (see Sect. 3). The participation of chlorine in LOEs is proven by a corresponding change in hydrocarbon pattern (Ramacher *et al.*, 1997).

In the beginning of April 1996 signals of up to 4 ppt are mainly assigned to RO_x/HO_x. The daily variation of the RO_x-box signals at that time followed the measured photolysis rates, $J(NO_2)$ in 1995 and $J(O_3(O^1D))$ in 1996. The situation was very similar to that at the end of May through June 1995. The RO_x-box signals disappeared at night which indicates a relatively short lifetime for RO_x/HO_x under those conditions. In 1995 the noon time maxima of the RO_x-box signals decreased from May to June 1995 (Fig. 5) though the radiative flux increased during that time period. Possibly the higher temperatures and the higher humidity caused a decrease of CHL_{perox} in the RO_x-box or the ambient O_3 concentrations were slightly lower.

During LOEs the lesser O_3 causes lower peroxy radical formation rates following the reaction of less OH with hydrocarbons. In the absence of O_3 and especially at low sun elevation the RO_x-box signals may therefore be caused by chlorine radicals. Whenever the signals exceeded 4 ppt RO_x/HO_x as found in the beginning of April, the higher signal could have been caused by ClO_x. The increases to up to 10 ppt (Figs. 5, 8) would indicate 3 ppt ClO_x at maximum, representing an upper limit for active chlorine found by us so far. Impey *et al.* (1997) reported several episodes of 30 ppt photolysable chlorine at Alert which were not significantly restricted to LOEs. In this work we find a strong connection to LOEs except for the episode April 14–19.

In the presence of O_3 and in bright daylight most of the active halogen is in the form of BrO and ClO due to the fast reaction of the halogen atoms with O_3. When O_3 disappears completely the active halogens are converted to the atomic form through reactions (2)–(4) and (8)–(12). Cl atoms quickly transform to HCl (see earlier) and the reaction of chlorine atoms with hydrocarbons also leads to the formation of RO_2. Though Br atoms do not react with methane they are converted moderately fast to HBr, Eqs. (31), (32). Therefore, in the morning of May 5, in the complete absence of O_3 as confirmed also by the absence of BrO, the RO_x-box signals could be due to leftover ClO and perhaps to some RO_2 produced by Cl atoms (Figs. 7, 8). The lifetime of RO_2 is usually not very long as pointed out above in the absence of LOEs. In the morning of May 6 and at midnight May 8/9 the presence of BrO indicates that O_3 was not completely destroyed. Consequently there should still be active chlorine in the form of OClO. The RO_x-box signals for those times may therefore indicate up to 2 ppt ClO_x, as

probably RO_x produced by the reactions of Cl atoms with hydrocarbons was negligible.
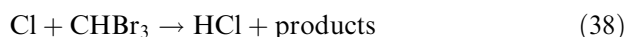
4.2 Halogen activation

The emission of the halogens in the Arctic could be started already in the dark by an activation of bromine by O_3 (Oum *et al.*, 1998a; Hirokawa *et al.*, 1998) or by an activation of chlorine, by far the most abundant halogen. For the latter the following mechanisms have been discussed in literature:

a. Impey *et al.* (1997) reported halogen production in dark Arctic regions. The chlorine and bromine may have been produced under the influence of O_3 from sea salt on the ice.
b. Oum *et al.* (1998b) found pure chlorine production from sea salt under the influence of O_3 and light. The short wave photolysis of O_3 may lead to OH which liberates Cl atoms from chlorides and then HOCl is formed via reactions (1) and (33).

Those primary production rates are not large enough to support the observed emission rates so that, in addition, autocatalytic processes have been claimed.

c. The HOCl oxidises sea salt halogenides to form Cl_2 and BrCl. The ongoing photolysis and reactions produce additional HOBr (Eq. 5) which then leads to the known autocatalytic bromine multiplication from abundant Br^- and Cl^-, which are found on aerosols or on the pack ice. The heterogeneous reactions (13), (35), (36) were first suggested by Fan and Jacob (1992) and further discussed by Mozurkewich (1995), Sander and Crutzen (1996), Vogt *et al.* (1996), Tang and McConnell (1996).
d. The importance of organic bromides as a starter of halogen chemistry or as major source for active bromine formation in the Arctic is not known. The seasonal variation of bromoform shows large mixing ratios in winter reaching average 10 ppt at Point Barrow, Alaska, compared with 2 ppt in summer (Cicerone *et al.*, 1988). Large concentrations of bromoform and other organic bromides have been reported for several places the Arctic by Berg *et al.* (1984). At Barrow they found up to 46 ppt. During a LOE at Alert Yokouchi *et al.* (1994) observed a doubling of bromoform mixing ratios from a background of 1.5 ppt and most interesting an exact negative correlation between O_3 and bromoform. A possibility could be the initiation of the autocatalytic bromine cycles through oxidation of bromoform by Cl atoms (Eq. 38):

$$Cl + CHBr_3 \rightarrow HCl + products \qquad (38)$$

However, a formation of bromoform during halogen activation and the intensive process of hydrocarbon oxidation involving chlorine in the presence of bromine should be considered as well.

Most experimental observations from ARCTOC point to process c as the the most important mechanism

for bromine liberation and O_3 destruction. High BrO and total bromine mixing ratios are observed during LOEs. Yet to a lesser extent ClO_x is involved also.

On May 5–6 and 8–9, 1996, in the presence of very little O_3 the RO_x-box signalled activated chlorine. Peroxy radicals formed via Cl-atom reactions with hydrocarbons but large radical yields on the basis of O_3 photochemistry were precluded by low O_3 mixing ratios. ClO_x mixing ratios could have been up to 3 ppt at maximum during day-time. At night from May 5 to May 9 signals corresponded to 0.5–1.5 ppt ClO_x. Chemical box model calculations including homogeneous processes only indicate a short overall lifetime of active chlorine due to its reaction with hydrocarbons (Eq. 28), so that its concentration should have been diminished during transport over open water from the higher values existing probably over the pack ice.

On one occasion a pure chlorine activation was observed. On April 14–20, 1996, non-zero RO_x-box signals at night (Fig. 8) and about 8 ppt peroxy radicals in the day-time were found while neither O_3 depletion nor BrO were observed. At the same time Ramacher *et al.* (1997) found a small decline of the nonmethane hydrocarbons, NMHC, from their anticipated behaviour. This observation under low wind conditions (Fig. 6) very likely shows a local primary activation of chlorine. The driving mechanism could have been the activation of chloride deposits on the snow in the Ny-Ålesund area, an oxidation of sea-salt as described by Oum *et al.* (1998b) or an oxidation by Caro's Acid as proposed by Mozurkewich (1995) as 300 ppt SO_2 were observed at the same time. In that period no spectroscopic sign of ClO was found neither by us nor by Tuckermann *et al.* (1997).

In 1995, when Spitsbergen was close to or part of the pack-ice layer, such events of active chlorine were observed more frequently (Fig. 5). Its mixing ratios according to the RO_x-box were of the same order of magnitude as in 1996. High night time signals were found on May 4/5, 11/12 and 12/13 (Fig. 5) together with indirect evidence for chlorine atoms (Ramacher *et al.*, 1997). BrO did not exceed the detection limit then, but slight decreases in O_3 were observed (Fig. 4) which seem to indicate a more advanced chlorine activation than on April 14–20, 1996, when O_3 was not found to be depleted. No RO_x-box measurements had been made during the LOE around April 20.

4.3 Total halogens

Total halogens have only been measured in 1996. The total bromine agrees very well with the amounts reported by Berg *et al.* (1983) and by Barrie *et al.* (1994). During normal periods ($O_3 \sim 45$ ppb) total bromine was 10 to 20 ppt which corresponds to the anticipated content of organobromides (mainly CH_3Br and halons) in the free northern troposphere (Schauffler *et al.*, 1998). Whenever BrO was observed, total bromine increased (Fig. 6) while the organic bromides did not vary strongly (Ramacher, private communication). The part of the total bromine

(Figs. 6, 7) which exceeds the sum of BrO and organobromides may be considered as inorganic, e.g. Br, Br_2, HOBr and HBr. On May 5, 1996, this part amounted to 28–33 ppt and may be compared with the 25 ppt "filterable" bromine found by Lehrer at Zeppelin station (ARCTOC, 1997). Impey *et al.* (1997) reported up to 40 ppt photolyzable bromine at Alert, which agrees widely with the calculated Br_2 and HOBr. However, their observations rarely showed a negative correlation of the photolyzable bromine with O_3.

In 1996 the first LOE began May 1–3 and mixing ratios of O_3, BrO and the wind speed of the oncoming air varied considerably. On May 4–9 the BrO increased to 20 ppt and O_3 was 0–15 ppb (Fig. 7). Total bromine was about 60 ppt corresponding to 40–50 ppt inorganic bromine. At noon of May 5, BrO read zero because O_3 was completely destroyed, while total bromine remained almost constant. Then a sharp maximum of 91 and 75 ppt total bromine followed. At approximately the same time SO_2 mixing ratios of more than 3 ppb (Fig. 7) were registered. Such a coincidence of SO_2 and very high total bromine was only observed on this occasion. This might be just a chance occurrence. However, it could as well indicate an additional activation of bromine by anthropogenic pollution. Mozurkewitch (1995) suggested that under conditions of low temperature and high SO_2 concentrations the free chain oxidation of S(IV) to produce peroxymonosulfuric acid, which oxidises bromide to elemental bromine. Furthermore, the air containing only SO_2 at the measurement site probably was polluted at an earlier stage by NO_2 and SO_2, as anthropogenic sources normally emit SO_2 and NO together. During the transport over the ice the NO_2 would have reacted with the early BrO to form bromine nitrate, $BrONO_2$ (39). The bromine nitrate then would have oxidised additional Br^- (40) to form Br_2 (Fan and Jacob, 1992).

$$BrO + NO_2 + M \rightarrow BrONO_2 + M \qquad (39)$$

$$BrONO_2 + Br^- \rightarrow Br_2 + NO_3^- \qquad (40)$$
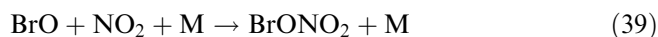
By the time the air arrived at Ny-Ålesund only SO_2 was left, as the NO_2 is removed effectively by reactions (39) and (38). In addition OH also reacts about an order of magnitude faster with NO_2 than with SO_2.

Total chlorine measured by neutron activation showed a very large variability due to sea-salt interference and no correlation with the ClO_x from the RO_x-box could be found.

Total iodine levels higher than the normal 1–2 ppt came together with high levels of total bromine: on April 25/26, 1996, 4 ppt iodine were detected together with 36 ppt bromine, and on May 6, 8 ppt iodine coincided with 75 ppt bromine (Fig. 6). Iodine is probably released in a similar way from sea-salt as bromine, i.e. in the form of ICl or IBr after iodide oxidation by HOCl or HOBr. IBr and ICl easily photolyse to I-atoms which react with O_3 (1) forming IO. The efficient photolysis of IO with a lifetime of only a few seconds at noon (Laszlo *et al.*, 1995) implies that iodine atoms may have represented a substantial fraction of the total iodine,

which could explain why IO was never detected even with a detection limit of 2 ppt. As a consequence only few IO radicals react with ClO (Bedjanian *et al.*, 1997) or BrO (Gilles *et al.*, 1997) and O_3 destruction by iodine is small. Also a formation of yet unknown and more stable iodine compounds cannot be excluded.

4.4 Low ozone events

The results support the suggestion that bromine plays a major role in the polar O_3 depletion (Barrie *et al.*, 1988).

Halogen atoms react with O_3 (1) to form the halogen monoxides which undergo cycles I to III and quickly destroy O_3. Loss of active halogen may be transformation into the respective hypohalogenous acids, strong oxidants (Eqs. 5, 33) or the formation of hydrohalogenic acids, HCl and HBr Eqs. (28), (31) and (32). HOCl and HOBr release or recycle halogenides for example from sea-salt heterogeneously to Cl_2, BrCl and Br_2 by reactions (13), (35) and (36). However, the rapid loss of active chlorine from the gas phase (Eq. 28) limits the effectiveness of chlorine (Lary, 1996; see also Sect. 4.2) and may explain why never more than 3 ppt ClO_x were found. So the efficient destruction of O_3 proceeds mainly through catalytic cycles I–II (see introduction). Iodine seems to be less important in the O_3 destruction cycles as explained already.

4.5 Box-model

BrO is exclusively and consistently detected during depletion events (except on occasions of thorough O_3 depletion). A simple chemical box model was developed using the program Facsimile and which included mainly bromine, chlorine and methane chemistry (DeMore *et al.*, 1997; Sander and Crutzen, 1996) to describe the measured BrO, ClO and total bromine. NO_x was not considered.

The model was initialised with 140 ppb CO and 1.88 ppm CH_4 (as measured by Ramacher *et al.*, 1997), 1.75‰ H_2O (90% relative humidity at 258 K) at 980 mb (average pressure along the lightpaths). Average values for the O_3 photolysis rate $J(O_3(O^1D)) = 5 \times 10^{-6} \, s^{-1}$ as obtained from Fig. 8 and $J(NO_2) = 8 \times 10^{-3} \, s^{-1}$ as measured at Zeppelin station (Monitor Lab; NILU) (Fig. 5) were used. The reactions included in the model are listed in Table 2 and the anticipated basic process is as follows.

As long as an airmass moves over the polar cap, heterogeneous oxidation of bromide and chloride on the pack-ice surface and on ice crystals eventually raised by the wind or formed by sublimation liberates active halogens to the atmosphere. O_3 will be depleted in the course of this process. The rate of the heterogeneous reaction depends largely on the surface available, which is not known. The overall value $k_{13} = 1 \times 10^{-11} \, cm^3 \, s^{-1}$ was arbitrarily chosen so that HBr becomes the rate limiting factor, as practically all HBr reacts immediately with HOBr, reforming Br_2 (Eq. 13). If ClO is included at permanent 2 ppt its influence on O_3 destruction is

Table 2. Reactions used in the model calculation

Reaction	J [s^{-1}] $k_{258\,K}$ [cm^3/s]	Reference
$Br + O_3 \rightarrow BrO + O_2$	7.7×10^{-13}	[b] (1)
$BrO + BrO \rightarrow 2Br + O_2$	2.8×10^{-12}	[b] (2)
$BrO + BrO \rightarrow Br_2 + O_2$	7.8×10^{-13}	[b] (3)
$Br_2 + h\nu \rightarrow 2Br$	3.6×10^{-2}	[f] (4)
$BrO + HO_2 \rightarrow HOBr + O_2$	2.8×10^{-11}	[b] (5)
$HOBr + h\nu \rightarrow Br + OH$	1.2×10^{-3}	[f*] (6)
$OH + O_3 \rightarrow HO_2 + O_2$	4.2×10^{-14}	[b] (7)
$HBr_{(aq)} + HOBr \rightarrow Br_2 + H_2O$	1.0×10^{-11}	[h] (13)
$OH + CO + O_2 \rightarrow HO_2 + CO_2$	2.4×10^{-13}	[b] (15)
$H + O_2 + M \rightarrow HO_2 + M$	1.7×10^{-12}	[b] (16)
CH_3O_2 $\quad + CH_3O_2 \rightarrow 2CH_3O + O_2$	1.6×10^{-13}	[b] (29)
$CH_3O + O_2 \rightarrow CH_2O + HO_2$	1.2×10^{-15}	[b] (30)
$O_3 + h\nu \rightarrow O(^1D) + O_2$	5×10^{-6}	[a] (40)
$H_2O_2 + h\nu \rightarrow 2OH$	2×10^{-6}	[c] (41)
$CH_3O_2H + h\nu \rightarrow CH_3O + OH$	2×10^{-6}	[d] (42)
$CH_2O + h\nu \rightarrow CO + H_2$	4.4×10^{-5}	[f] (43)
$CH_2O + h\nu \rightarrow CO + 2HO_2$	2×10^{-5}	[f] (44)
$BrO + h\nu \rightarrow Br + O(^3P)$	4×10^{-2}	[e] (45)
$O(^1D) + H_2O \rightarrow 2OH$	2.2×10^{-10}	[b] (46)
$O(^1D) + O_2 \rightarrow O(^3P) + O_2$	4.2×10^{-11}	[b] (47)
$O(^1D) + N_2 \rightarrow O(^3P) + N_2$	2.8×10^{-11}	[b] (48)
$O(^1D) + H_2 \rightarrow OH + H$	1.1×10^{-10}	[b] (49)
$O(^3P) + O_2 + M \rightarrow O_3 + M$	2.3×10^{-14}	[b] (50)
$OH + H_2 \rightarrow H_2O + H$	2.4×10^{-15}	[b] (51)
$OH + OH + M \rightarrow H_2O_2 + M$	6.8×10^{-12}	[b] (52)
$OH + HO_2 \rightarrow H_2O + O_2$	1.3×10^{-10}	[b] (53)
$OH + H_2O_2 \rightarrow HO_2 + H_2O$	1.6×10^{-12}	[b] (54)
$HO_2 + O_3 \rightarrow OH + 2O_2$	1.6×10^{-15}	[b] (55)
$HO_2 + HO_2 \rightarrow H_2O_2 + O_2$	2.4×10^{-12}	[b] (56)
$HO_2 + HO_2 + M \rightarrow H_2O_2$ $\qquad + O_2 + M$	2.3×10^{-12}	[b] (57)
$OH + CH_4 \rightarrow CH_3 + H_2O$	2.5×10^{-15}	[b] (58)
$CH_3 + O_2 + M \rightarrow CH_3O_2 + M$	1.6×10^{-12}	[b] (59)
$CH_2O + OH \rightarrow HCO + H_2O$	1.0×10^{-11}	[b] (60)
$CH_3OH + OH \rightarrow CH_2OH + H_2O$	6.5×10^{-13}	[b] (61)
$OH + CH_3O_2H \rightarrow CH_3O_2 + H_2O$	5.9×10^{-12}	[b] (62)
$OH + CH_3O_2H \rightarrow CH_2O$ $\qquad + OH + H_2O$	2.4×10^{-12}	[b] (63)
$HO_2 + CH_3O_2 \rightarrow CH_3O_2H + O_2$	8.4×10^{-12}	[b] (64)
$HCO + O_2 \rightarrow CO + HO_2$	6.0×10^{-12}	[b] (65)
$CH_2OH + O_2 \rightarrow CH_2O + HO_2$	9.1×10^{-12}	[b] (66)
CH_3O_2 $\quad + CH_3O_2 \rightarrow CH_3O_2CH_3 + O_2$	5.2×10^{-14}	[b] (67)
CH_3O_2 $\quad + CH_3O_2 \rightarrow CH_2O + CH_3OH + O_2$	3.1×10^{-13}	[b] (68)
$Br_2 + OH \rightarrow HOBr + Br$	4.2×10^{-11}	[b] (69)
$BrO + OH \rightarrow Br + HO_2$	7.5×10^{-11}	[b] (70)
$HBr + OH \rightarrow H_2O + Br$	1.1×10^{-11}	[b] (71)
$Br + HO_2 \rightarrow HBr + O_2$	1.5×10^{-12}	[b] (72)
$Br + CH_2O \rightarrow HBr + HCO$	7.7×10^{-13}	[b] (73)
$BrO + CH_3O_2 \rightarrow Br + CH_3O + O_2$	1.0×10^{-11}	[g] (74)

[a] measured
[b] DeMore *et al.* (1997)
[c] photolysis rate from (DeMore *et al.*, 1997) scaled on J(O^{1}D)
[d] photolysis rate from (Sander and Crutzen, 1996), scaled on J(O^{1}D)
[e] photolysis rate from (DeMore *et al.*, 1997) scaled on J(NO$_2$)
[f] photolysis rate from (Sander and Crutzen, 1996), scaled on J(NO$_2$)
[f*] as f, multiplied by a factor 2 (Barnes *et al.*, 1996)
[g] J. Crowley, 1997, personal communication
[h] hetrogeneous reaction (Fan and Jacob, 1992)

negligible. Therefore, chlorine reactions were omitted in the following estimate.

Figure 12 shows O_3 and bromine compounds for an initial Br_2 mixing ratio of 25 ppt. Reduction of the initial $\sim$45 ppb O_3 to $\sim$5 ppb takes about 4 days, with constant 15 to 20 ppt BrO. This is not in agreement with the measured data, as for specific O_3 mixing ratios variable BrO mixing ratios were registered (Fig. 11). Apparently additional processes got involved with the pure chemistry (see 4.6 Transport model). After total destruction of O_3 the bromine is firstly converted to Br and Br_2 and then slowly to HBr.

4.6 Transport model

The large disagreement of the box model simulation with our field data is not surprising since the simulation describes the situation on the ice cap, whereas especially during the 1996 campaign, several hundred kilometres of open water separated Ny-Ålesund from the pack-ice region.

As shown in Fig. 10, the O_3 is negatively correlated with total bromine: the O_3 content of the air decreases linearly with its amount of bromine, beginning at values of about 15 ppt, corresponding to the estimated background organic bromine, and reaching zero for about 50 ppt additional bromine. A negative correlation is expected for an airmass in which the O_3 has been depleted according to its bromine content, as more bromine leads to a faster O_3 depletion and therefore the O_3 mixing ratio observed after a certain amount of time should decrease.

However, it should be noted that the O_3 depletion rate in principle is not linearly proportional to the total bromine content of the air, therefore the observed linearity of the ozone/bromine relation is remarkable.

The rate of the O_3 destruction is controlled by the self-reaction of BrO, Eqs. (2), (3), the reaction of BrO
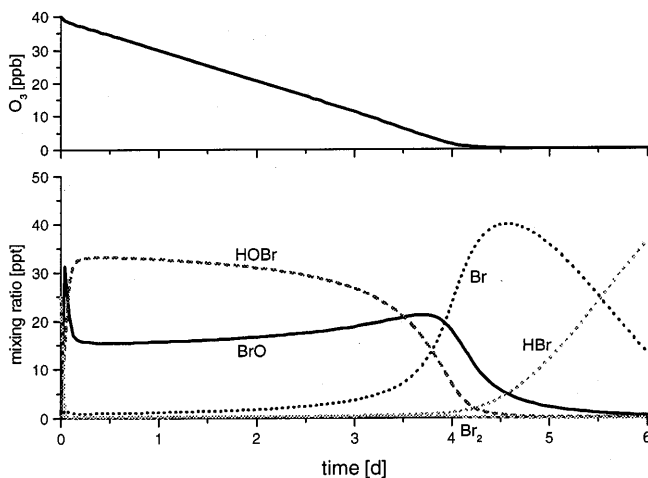
Fig. 12. Model calculation: time-dependent development of O_3 and bromine compounds assuming a rapid heterogeneous oxidation of Br$^-$ by HOBr on the ice cap forming Br_2

with HO_2, Eq. (5), and the reactions of BrO with ClO, Eqs. (8), (9), followed by the photolysis of the products, Eqs. (4), (6), and (11). As chlorine reactions are of minor importance it is implied that the ozone destruction rate is proportional to the HOBr concentration and to the square of the BrO concentration:

$$\frac{dO_3}{dt} = 2 \cdot [BrO]^2 \cdot k_{BrO+BrO} + 2[HOBr] \, J_{HOBr} \tag{41}$$

The BrO and HOBr concentrations in the modelled system are proportional to the total inorganic bromine, as can be verified by changing the initial Br_2 mixing ratio. For the simulation shown in Fig. 13 the initial Br_2 mixing ratio was halved to 12.5 ppt compared with the 25 ppt used for the simulation given in Fig. 12. BrO and HOBr then also appear by a factor of 2 smaller than in Fig. 12. The O_3 depletion rate in Fig. 13 on the contrary is almost a factor of 3 lower, as its dependence on bromine is nonlinear Eq. (41).

The ozone/bromine relation also depends on the duration of the O_3 depletion since the input of bromine. The actual rate of bromine release in the Arctic is unknown. The model scenario corresponds to a rapid bromine release, the O_3 destruction taking place afterwards at a relatively constant bromine mixing ratio. The O_3 loss after a given time is proportional to the approximately constant O_3 depletion rate, which is not linearly proportional to the bromine mixing ratio, as shown already. Additionally, the wind speed during the O_3 depletion event, which lasted for several days, varied considerably between 0 and almost 10 m/s. Substantially different transport times from the bromine source and therefore different durations of O_3 depletion in the observed airmasses can be expected. This should lead to considerable scatter, whereas relatively little scatter was actually observed.

In the model scenario the initial bromine concentration corresponds to the bromine content observed at Ny-Ålesund. However, if the rate of bromine release was slow, the O_3 destruction would have been caused by a lower average bromine level than that finally observed at
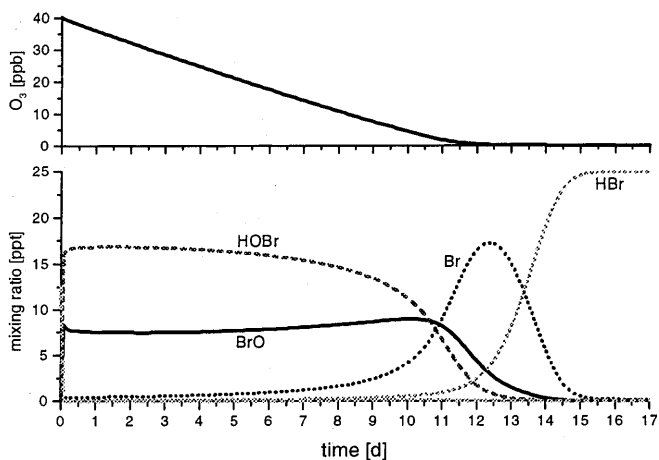
Fig. 13. Model calculation: analogous to Fig. 12, time-dependent development of O_3 and bromine compounds including heterogeneous oxidation but for only half of the initial bromine compared to Fig. 12

the measurement site. The bromine in the air increases probably exponentially due to the autocatalytical process as long as there is no limitation by the available bromide.

In short, many factors which are not linearly dependant on the bromine amount observed at the site of measurement will influence the process of O_3 depletion. Therefore additional mechanisms presumably lead to the observed linear correlation of O_3 loss and bromine concentration. One important possibility is mixing, as the transport of cold air over the warmer open water is likely to lead to mixing with upper air rich in O_3. Additional mixing occurs at the boundaries of a depleted airmass. The observed linear negative correlation could be caused by mixing of air thoroughly deprived of O_3 to various degrees with air rich in O_3. In this case the relation of O_3 and total bromine determines the extent of that mixing (Fig. 10).

During transport over the open sea heterogeneous reactions should be reduced, so that the O_3 destruction in the mixed air is not as effective as that before over the ice. For a rough comparison of the relative importance of heterogeneous reactions over the pack ice and over the open sea it is assumed that the surface of the ice crystals kept aloft by the wind corresponded to the area of the ice-covered ground. In a mixing layer of 1000 m the ice crystals then should provide a surface of about $1000 \, \mu m^2/cm^3$. However, measurements by Staebler (ARCTOC, 1992) showed that the average aerosol surface area at Zeppelin station during the campaign in 1996 was only $40 \, \mu m^2/cm^3$. Heterogeneous reactions therefore became slower by about a factor of 25 after the airmass left the pack ice.

To simulate the behaviour of this system during transport, the heterogeneous reaction was removed from the model. Bromine and O_3 values were taken from Fig. 10, assuming that the air coming to Ny-Ålesund was a mixture of two airmasses, one with no O_3 and about 25 ppt Br_2 at the time of mixing, the other with about 40 ppb O_3 and no inorganic bromine.

As soon as the two airmasses are mixed, BrO forms, as shown in Fig. 14, and bromine is converted to HOBr and HBr within roughly one day. The initial amount of BrO and also the conversion rate of BrO to HOBr and of Br to HBr depend on the degree of mixing with O_3 rich air. The BrO observed is a strong function of transport time (Figs. 14, 15) and therefore the BrO for a given O_3 and total bromine mixing ratio will vary with wind speed. During the main O_3 depletion event in 1996 transport times between 3 and 9 h are given by the trajectories (A. Rasmussen, personal communication). According to the model the highest BrO levels are then expected for 5 ppb O_3 (Fig. 15), which is in agreement with the observations (see Fig. 11). The increase towards the maximum at low O_3 levels is dominated by the O_3 limited formation of BrO from bromine atoms through reaction (1) and the decrease towards higher O_3 levels by mixing.

In 1995 the ice edge was close to Ny-Ålesund, and air from northerly directions did not pass over open water. During the LOE the air came mostly from the northeast
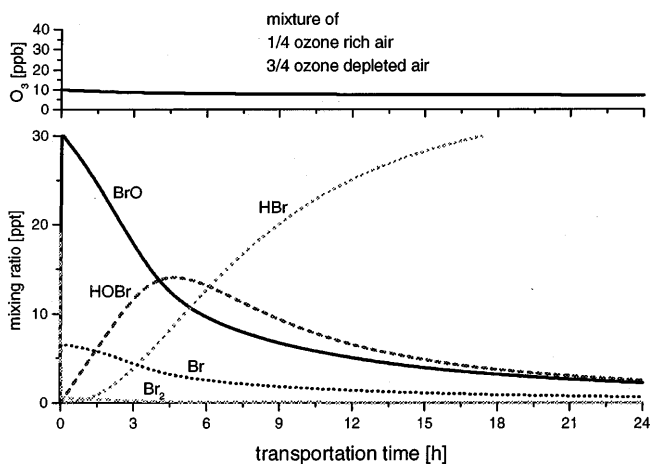
Fig. 14. Model calculation: time dependent development of O_3 and bromine compounds for a mixed airmass and no heterogeneous chemistry

but had to pass over parts of Spitsbergen, where mixing was induced by orographic structures. This mixing with upper air is likely to have started about 1–3 h before the air arrived at the measurement site. As total bromine was not measured in 1995, a detailed analysis cannot be performed. Nevertheless, assuming the total inorganic bromine amount to be close to that of 1996, the high BrO levels of up to 30 ppt are consistent with the more recent mixing which explains as well the frequent observation of high amounts of ClO_x in 1995.

4.7 Estimation of the inorganic bromine source strength

The bromine emission from the pack-ice can be estimated. Back-trajectories suggest that the air observed during the first O_3 depletion event in 1996, containing 50 ppt inorganic bromine, had been transported over the pack-ice for approximately 5 days. If, as
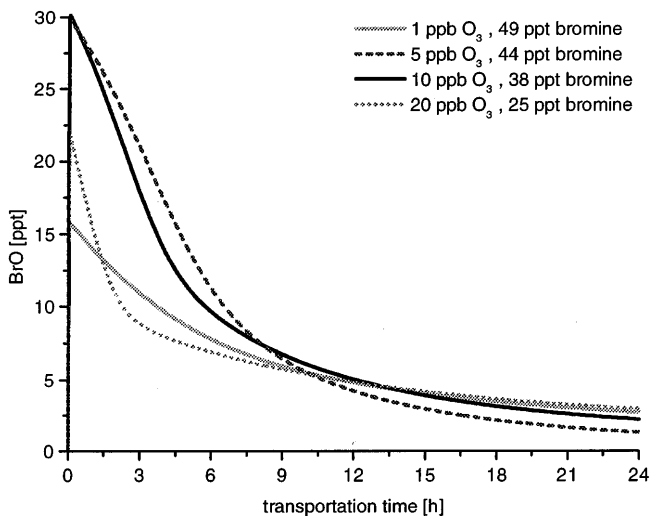
Fig. 15. Model calculation: development of BrO with time for various mixtures of O_3 depleted air containing 25 ppt Br_2 with background air containing 40 ppb O_3 and no bromine

suggested by Fan and Jacob (1992), the bromine is released by HOBr oxidation of sea-salt bromide, the bromine emission will stop as soon as the O_3 disappears. The same argument holds for chlorine. Therefore the bromine mixing ratio in a thoroughly O_3 depleted airmass above the pack-ice will be always similar and must be independent of the mixing height. During the depletion event the mixed layer at the measurement site was about 2 km high (ARCTOC, 1997), indicating a corresponding height above the pack-ice. Constant bromine emission giving a total of 50 ppt after 5 days in a mixed layer of 1000 m requires a bromine emission rate of 3.5×10^{12} Br-atoms $m^{-2} s^{-1}$. In average the mixing layer height over the pack-ice in spring and summer is only about 300 m (Serreze *et al.*, 1992), resulting in an estimated bromine emission rate of about 1×10^{12} Br-atoms $m^{-2} s^{-1}$, if we assume an air mass exchange every 5 days. This emission rate throughout spring and summer on an average pack-ice area of 1×10^7 km^2 in the Arctic and of 4×10^6 km^2 in the Antarctic then leads to an estimated inorganic bromine source strength of about 30 kt y^{-1} from polar regions.

5 Summary

O_3 depletion is driven by photochemical destruction involving bromine and to a minor extent chlorine atoms as well. The starting process probably releases Br_2, BrCl from sea-salt on the ice cap in unpolluted air. This is followed by autocatalytic halogen emission, i.e. increasing heterogeneous recycling and release of halogens presumably from ice/sea-salt surfaces, and concurrent O_3 destruction. The halogen emission process should supposedly end when the O_3 is depleted. The negative linear correlation of the total bromine and O_3 data obtained during a strong O_3 depletion event and the large variability of the measured BrO data is in agreement with the hypothesis that O_3 depleted airmasses mix with O_3 rich air on leaving the ice cap. In this case the BrO values observed at the measurement site were controlled by gas-phase chemistry and mixing.

Very high total bromine values coincided with enhanced SO_2 and support the hypothesis that anthropogenic pollution enhances the bromine release rate through additional heterogeneous oxidation of Br^- by peroxymonosulfuric acid or by $BrONO_2$.

In addition to the peroxy radicals produced by OH photooxidation cycles of hydrocarbons the RO_x-box signals are caused also by ClO_x. This is indicated by higher RO_x-box signals, especially at night. Active chlorine is most frequently observed during O_3 depletion events but sometimes also under otherwise undisturbed conditions. The ClO_x mixing ratio at the measurement site did not exceed 2–3 ppt. The overall bromine emission rate is estimated for sunlit pack-ice as 1×10^{12} molec. Br m$^{-2} s^{-1}$.

References

ARCTOC, Arctic Tropospheric Ozone Chemistry, Results from field, laboratory and modelling studies, *Final Report to European Union* (Ed. U. Platt and E. Lehrer), Europ. Comm. Air Pollution Report, 64, 1997.

Arnold, T., *Die Rolle von Peroxyradikalen bei atmosphärischen Oxidationsprozessen*, Dissertation, Gutenberg Universität, Mainz, 1998.

Barrie, L. A., J. W. Bottenheim, R. C. Schnell, P. J. Crutzen, and R. A. Rasmussen, Ozone destruction and photochemical reactions at polar sunrise in the lower arctic atmosphere, *Nature*, **334,** 138–141, 1988.

Barrie, L. A., G. den Hartog, J. W. Bottenheim, and S. Landsberger, Anthropogenic aerosols and gases in the lower troposphere at Alert, Canada, in April 1986, *J. Atmos. Chem.*, **9,** 101–127, 1989.

Barrie, L. A., S.-M. Li, D. L. Toom, S. Landsberger, and W. Sturges, Lower tropospheric measurements of halogens, nitrates and sulphur oxides during Polar Sunrise Experiment 1992, *J. Geophys. Res.*, **99,** 25 453–25 468, 1994.

Bass, A. M., and R. J. Paur, The ultraviolet cross-sections of ozone, *Proc. Quadrennial Ozone Symposium*, Greece (Ed. C. Zerefos and A. Ghazi), 606–617, 1984.

Bedjanian, Y., G. Le Bras, and G. Poulet, Kinetics and mechanism of the IO + ClO reaction, *J. Phys. Chem.*, **101,** 4088–4096, 1997.

Behnke, W., M. Elend, U. Krüger, and C. Zetsch, Promotion and inhibition of the Br^- catalysed production of halogenated radicals from the gas-phase interaction with sea-salt aerosols, *Proc. Eurotrac-2 Symposium*, 23–27 March 1998, Garmisch Partenkirchen, Ed. P. Borrell, 1998.

Berg, W. W., P. D. Sperry, K. A. Rahn, and E. S. Gladny, Atmospheric bromine in the Arctic, *J. Geophys. Res.*, **88,** 6719–6736, 1983.

Berg, W. W., L. E. Heidt, W. Pollock, P. D. Sperry, K. A. Rahn, and R. J. Cicerone, Brominated organic species in the Arctic atmosphere, *Geophys. Res. Lett.*, **11,** 429–432, 1984.

Bongartz, A., J. Kames, F. Welter, and U. Schurath, Near-UV absorption cross sections and trans/cis equilibrium of nitrous acid, *J. Phys. Chem.*, **95,** 1076–1082, 1991.

Bongartz, A., J. Kames, U. Schurath, C. George, P. Mirabel, and J. L. Ponche, Experimental determination of HONO mass accomodation coefficients using two different techniques, *J. Atmos. Chem.*, **18,** 149–169, 1994.

Bottenheim, J. W., A. J. Gallant, and K. A. Brice, Measurements of NO_y species and O_3 at 82°N latitude, *Geophys. Res. Lett.*, **13,** 113–116, 1986.

Bottenheim, J. W., L. W. Barrie, E. Atlas, L. E. Heidt, H. Niki, R. A. Rasmussen, and P. B. Shepson, Depletion of lower tropospheric ozone during arctic spring: the Polar Sunrise Experiment 1988, *J. Geophys. Res.*, **95,** 18 555–18 568, 1990.

Brauers, T., M. Hausmann, U. Brandenburger, and H. -P. Dorn, Improvement of differential optical absorption spectroscopy with a multichannel scanning technique, *Appl. Optics*, **34,** 4472–4479, 1995.

Brune, W. H., P. S. Stevens, and J. H. Mather, Measuring OH and HO_2 in the troposphere by laser-induced fluorescence at low pressure, *J. Atmos. Sci.*, **52,** 3328–3336, 1995.

Cantrell, C. A., D. H. Stedman, and G. J. Wendel, Measurement of atmospheric peroxy radicals by chemical amplification, *Anal. Chem.*, **56,** 1496–1502, 1984.

Cicerone R. J., L. E. Heidt, and W. H. Pollock, Measurements of atmospheric methyl bromide and bromoform, *J. Geophys. Res.*, **93,** 3745–3749, 1988.

de Serves, C., Gas phase formaldehyde and peroxide measurements in the Arctic atmosphere, *J. Geophys. Res.*, **99,** 25 391–25 398, 1994.

DeMore, W. B., S. P. Sander, D. M. Golden, R. F. Hampson, M. J. Kurylo, C. J. Howard, A. R. Ravishankara, C. E. Kolb, and M. J. Molina, Chemical kinetics and photochemical data for use in stratospheric modeling, *JPL Publication*, 97-4, 1997.

Eigen, M., and K. Kustin, The kinetics of halogen hydrolysis, *J. Am. Chem. Soc.*, **84,** 1355–1361, 1962.

Fan, S.-M., and D. J. Jacob, Surface ozone depletion in Arctic spring sustained by bromine reactions on aerosols, *Nature*, **359,** 522–524, 1992.

Fickert S., J. Adams, G. K. Moortgat, and J. N. Crowley, Release of Br_2 and BrCl by heterogeneous reaction of HOBr on sea-salt aerosol, *Proc. Eurotrac-2 Symposium*, 23–27, March 1998, Garmisch Partenkirchen, Ed. P. Borrell, 1998.

Finlayson-Pitts, B. J., F. E. Livingston, and H. N. Berko, Ozone destruction and bromine photochemistry at ground level in the Arctic spring, *Nature*, **343,** 622–624, 1990.

Gilles, M. K., A. A. Turnipseed, J. B. Burkholder, A. R. Ravishankara, and S. Solomon, Kinetics of the IO radical. 2. Reaction of IO with BrO, *J. Phys. Chem.*, **101,** 5526–5534, 1997.

Hastie, D. R., M. Weißenmayer, J. P. Burrows, and G. W. Harris, Calibrated chemical amplifier for atmospheric RO_x measurements, *Anal. Chem.*, **63,** 2048–2057, 1991.

Hausmann, M. and U. Platt, Spectroscopic measurement of bromine oxide and ozone in the high arctic during Polar Sunrise Experiment 1992, *J. Geophys. Res.*, **99,** 25 399–25 414, 1994.

Hewitt, A. D., K. M. Brahan, G. D. Boone, and S. A. Hewitt, Kinetics and mechanism of the Cl + CO reaction in air, *Int. J. Chem. Kin.*, **28,** 763–771, 1996.

Hirokawa, J., K. Onaka, Y. Kajii, and H. Akimoto, Heterogeneous processes involving sodium halide particles and ozone: molecular bromine release in the marine boundary layer in the absence of nitrogen oxides, *Geophys. Res. Lett.*, **25,** 2449–2452, 1998.

Hofzumahaus, A., T. Brauers, U. Aschmutat, U. Brandenburger, H.-P. Dorn, M. Hausmann, M. Heßling, F. Holland, C. Plass-Dülmer, M. Sedlacek, M. Weber, and D.H. Ehhalt, Reply to Lanzendorf, E. J., T. F. Hanisco, N. M. Donahue, and P. O. Wennberg, Comment on: "The measurement of tropospheric OH radicals by laser-induced fluorescence spectroscopy during the POPCORN field campaign" by Hofzumahaus *et al.* and "Intercomparison of tropospheric OH radical measurements by multiple folded long-path laser absorption and laser-induced fluorescence" by Brauers *et al.*, *Geophys. Res. Lett.*, **24,** 3039–3040, 1997.

Impey, G. A., P. B. Shepson, D. R. Hastie, L. A. Barrie, and K. G. Anlauf, Measurements of photolyzable chlorine and bromine during the polar sunrise experiment 1995, *J. Geophys. Res.*, **102,** 16 005–16 010, 1997.

Jobson, B. T., H. Niki, Y. Yokouchi, J. W. Bottenheim, F. Hopper, and W. R. Leaitch, Measurements of C_2—C_6 hydrocarbons during the polar sunrise 1992 experiment: evidence for Cl atom and Br atom chemistry, *J. Geophys. Res.*, **99,** 25 355–25 368, 1994.

Junkermann, W., U. Platt, and A. Volz-Thomas, A photoelectric detector for the measurement of photolysis frequencies of ozone and other atmospheric molecules, *J. Atmos. Chem.*, **8,** 203–227, 1989.

Kirchner, U. T. Benter, and R. N. Schindler, Experimental verification of gas phase enrichment in reactions of HOBr with sea salt doped ice surfaces, *Ber. Bunsenges. Phys. Chem.*, **101,** 975–977, 1997.

Kreher, K., *Spectroscopic measurements of atmospheric OClO, BrO and NO_2 and their relation to Antarctic ozone depletion*, Dissertation, Ruprecht-Karls Universität, Heidelberg, 1996.

Kreher, K., P. V. Johnston, S. W. Wood, B. Nardi, and U. Platt, Ground-based measurements of tropospheric and stratospheric BrO at Arrival Heights, Antarctica, *Geophys. Res. Lett.*, **24,** 3021–3024, 1997.

Ladstätter-Weißenmayer, A., Spektroskopische Untersuchungen von photochemischen Prozessen in der Atmosphäre unter

besonderer Berücksichtigung von Stickstoffverbindungen, Dissertation, Universität Mainz, 1992.

Lary, D. J., Gasphase atmospheric bromine photochemistry, *J. Geophys. Res.*, **101**, 1505–1516, 1996.

Laszlo, B., M. J. Kurylo, and R. E. Huie, Absorption cross sections, kinetics of formation, and self-reaction of the IO radical produced via laser photolysis of $N_2O/I_2/N_2$ mixtures, *J. Phys. Chem.*, **99**, 11 701–11 707, 1995.

Le Bras, G., and U. Platt, A possible mechanism for the combined chlorine and bromine catalysed destruction of tropospheric ozone in the Arctic, *Geophys. Res. Lett.*, **22**, 599–602, 1995.

Martinez, M., Messungen von BrO und anderen Spurenstoffen in der bodennahen Troposphäre, Dissertation, Ruprecht-Karls Universität, Heidelberg, 1998.

McConnell, J. C., G. S. Henderson, L. Barrie, J. Bottenheim, H. Niki, C. H. Langford, and E. M. J. Templeton, Photochemical bromine production implicated in Arctic boundary-layer ozone depletion, *Nature*, **355**, 150–152, 1992.

McElroy, M. B., R. J. Salawitch, S. C. Wofsy and J. A. Logan, Antarctic ozone: reductions due to synergistic interactions of chlorine and bromine, *Nature*, **321**, 759–762, 1986.

McGee, T. J., and J. Burris, SO_2 absorption cross section in the near U.V., *J. Quant. Spectrosc. Radiat. Transfer*, **37**, 165–182, 1987.

Mickle, R. E., J. W. Bottenheim, R. W. Leaitch, and W. Evans, Boundary layer ozone depletion during AGASP-II, *Atmos. Environ.*, **23**, 2443–2449, 1989.

Mihele, C. M., and D. R. Hastie, The sensitivity of the radical amplifier to ambient water vapour, *Geophys. Res. Lett.*, **25**, 1911–1913, 1998.

Mikkelsen, L. S., A. Rasmussen, J. H. Sørensen, and A. Weaver, Surface ozone observations over Greenland, *Europ. Geophys. Soc., XXI General Assembly*, vol. II of Abstr, C606, The Hague, The Netherlands, 6–10 May, 1996.

Miller, H. L., A. Weaver, R. W. Sanders, K. Arpag, and S. Solomon, Measurements of Arctic sunrise surface ozone depletion events at Kangerlussuaq, Greenland, *Tellus*, **49B**, 496–509, 1997.

Moortgat, G. K., and W. Schneider, *J. Phys. Chem. Ref. Data*, **18**, 1014, 1989.

Mozurkewich, M., Mechanisms for the release of halogens from sea-salt particles by free radical reactions, *J. Geophys. Res.*, **100**, 14 199–14 207, 1995.

Murayama, S., T. Nakazawa, M. Tanaka, S. Aoki, and S. Kawaguchi, Variations of tropospheric ozone concentration over Syowa station, Antarctica, *Tellus*, **44B**, 262–272, 1992.

Oltmans, S. J., and W. D. Komhyr, Surface ozone distributions and variations from 1973 to 1984 measurements at the NOAA Geophysical Monitoring for Climatic Change Baseline observatories, *J. Geophys. Res.*, **91**, 5229–5236, 1986.

Oum, K. W., M. J. Lakin, and B. J. Finlayson-Pitts, Bromine activation in the troposphere by the dark reaction of O_3 with seawater ice, *Geophys. Res. Lett.*, **25**, 3923–3926, 1998a.

Oum, K. W., M. J. Lakin, D. O. DeHaan, T. Brauers, and B. J. Finlayson-Pitts, Formation of molecular chlorine from the photolysis of ozone and aqueous sea-salt particles, *Science*, **279**, 74–77, 1998b.

Perner, D., T. Arnold, J. Crowley, T. Klüpfel, M. Martinez, and R. Seuwen, The measurement of active chlorine in the atmosphere by chemical amplification, *J. Atmos. Chem.*, in press 1999.

Platt, U., Differential optical absorption spectroscopy (DOAS), in *Air monitoring by spectroscopic techniques*, Ed. M.W. Sigrist, Chemical Analysis Series, **127**, John Wiley and Sons, 1994.

Platt, U., and D. Perner, Measurements of atmospheric trace gases by long path differential UV/visible absorption spectroscopy, optical and laser remote sensing (Ed. D. K. Killinger and A. Mooradien), *Springer Ser. Optical Sci.*, **39**, 95–105, 1983.

Ramacher, B., J. Rudolph, and R. Koppmann, Hydrocarbon measurements in the spring arctic troposphere during the ARCTOC 95 campaign, *Tellus*, **49B**, 466–485, 1997.

Rudolph, J., B. Ramacher, C. Plass-Dülmer, K.-P. Müller and R. Koppmann, The indirect determination of chlorine atom con-

centration in the troposphere from changes in the patterns of non-methane hydrocarbons, *Tellus*, **49B**, 592–601, 1997.

Sander, R., and P. J. Crutzen, Model study indicating halogen activation and ozone destruction in polluted air masses transported to the sea, *J. Geophys. Res.*, **101**, 9121–9138, 1996.

Schauffler, S. M., E. L. Atlas, F. Flocke, R. A. Lueb, V. Stroud and W. Travnicek, Measurements of bromine containing organic compounds at the tropical tropopause, *Geophys. Res. Lett.*, **25**, 317–320, 1998.

Schneider, W., G. K. Moortgat, G. S. Tyndall, and J. P. Burrows, Absorption cross-sections of NO_2 in the UV and visible region (200–700 nm) at 298 K, *J. Photochem. Photobiol.*, **40**, 195–217, 1987.

Schultz, M., M. Heitlinger, D. Mihelcic, and A. Volz-Thomas, Calibration source for peroxy radicals with built-in actinometry using H_2O and O_2 photolysis at 185 nm, *J. Geophys. Res.*, **100**, 18 811–18 816, 1995.

Serreze, M. C., J. D. Kahl, and R. C. Schnell, Low-level temperature inversions of the Eurasian Arctic and comparisons with soviet drifting station data, *Am. Meteorol. Soc.*, **5**, 615–629, 1992.

Simon, F. G., W. Schneider, G. K. Moortgat, and J. P. Burrows, A study of the ClO absorption cross-section between 240 and 310 nm and the kinetics of the self-reaction at 300 K. *J. Photochem. Photobiol. A: Chem.*, **55**, 1–23, 1990.

Solberg, S., N. Schmidtbauer, A. Semb, F. Stordal, and O. Hov, Boundary layer ozone depletion as seen in the Norwegian Arctic in spring, *J. Atmos. Chem.*, **23**, 301–322, 1996.

Sturges, W. T., R. C. Schnell, G. S. Dutton, S. R. Garcia, and J. A. Lind, Spring measurements of tropospheric bromine at Barrow, Alaska, *Geophys. Res. Lett.*, **20**, 201–204, 1993.

Stutz, J., *Messung der Konzentration troposphärischer Spurenstoffe mittels Differentieller-Optischer-Absorptionsspektroskopie: Eine neue Generation von Geräten und Algorithmen*, Dissertation, Ruprecht-Karls Universität, Heidelberg, 1995.

Tang, T., and J. C. McConnell, Autocatalytic release of bromine from Arctic snow pack during polar sunrise, *Geophys. Res. Letts.*, **23**, 2633–2636, 1996.

Tuckermann, M., R. Ackermann, C. Gölz, H. Lorenzen-Schmidt, T. Senne, J. Stutz, B. Trost, W. Unold, and U. Platt, DOAS-observation of halogen radical-catalysed arctic boundary layer ozone destruction during the ARCTOC-campaigns 1995 and 1996 in Ny-Alesund, Spitsbergen, *Tellus*, **49B**, 533–555, 1997.

Vogt, R., P. J. Crutzen, and R. Sander, A mechanism for halogen release from sea-salt aerosol in the remote marine boundary layer, *Nature*, **383**, 327–330, 1996.

Wahner, A., G. S. Tyndall, and A. R. Ravishankara, Absorption cross sections for OClO as a function of temperature in the wavelength range 240–480 nm, *J. Phys. Chem.*, **91**, 2734–2738, 1987.

Wahner, A., A. R. Ravishankara, S. P. Sander, and R. R. Friedl, Absorption cross section of BrO between 312 and 385 nm at 298 and 223 K, *Chem. Phys. Letts.*, **152**, 507–512, 1988.

Wessel, S., *Troposphärische Ozonvariationen in Polarregionen*, Dissertation, Universität Bremen, 1996.

Wessel, S., S. Aoki, R. Weller, A. Herber, H. Gernandt, and O. Schrems, Aerosol and ozone observations in the polar troposphere at Spitsbergen in spring 1994, *Atmos. Res.*, **44**, 175–189, 1997.

Wessel, S., S. Aoki, P. Winkler, R. Weller, A. Herber, H. Gernandt and O. Schrems, Tropospheric ozone depletion in polar regions: A comparison of observations in the Arctic and Antarctic, *Tellus*, **50B**, 34–50, 1998.

Wittrock, F., M. Eisinger, A. Ladstätter-Weißenmayer, A. Richter, and J. P. Burrows, Ground-based UV/VIS measurements of O_3, NO_2, OClO and BrO over Ny-Ålesund (79°N, 12°E), *Proc. XVIII Quadrennial Ozone Symposium, L'Aquila, Italy, 12–21 September 1996* (Eds. R.D. Bojkov and G. Visconti), 623–626, 1996.

Yokouchi, Y., H. Akimoto, L. A. Barrie, J. W. Bottenheim, K. Anlauf, and B. T. Jobson, Serial gas chromatographic/mass spectrometric measurements of some volatile organic compounds in the Arctic atmosphere during the 1992 Polar Sunrise Experiment, *J. Geophys. Res.*, **99**, 25 379–25 389, 1994.